PNAS RESEARCH ARTICLE | ENVIRONMENTAL SCIENCES CHEMISTRY

Diversity and evolution of nitric oxide reduction in bacteria and archaea

Ranjani Murali[a,b,c,1,2,3], Laura A. Pace[a,d], Robert A. Sanford[e], L. M. Ward[f,g], Mackenzie M. Lynes[h,i], Roland Hatzenpichler[h,ij], Usha F. Lingappa[g,k], Woodward W. Fischer[g], Robert B. Gennis[a], and James Hemp[d,g,1,2]

Affiliations are included on p. 7.

Edited by José J. Moura, Universidade Nova de Lisboa, Caparica, Portugal; received September 27, 2023; accepted April 24, 2024 by Editorial Board Member Marcetta Y. Darensbourg

Nitrous oxide is a potent greenhouse gas whose production is catalyzed by nitric oxide reductase (NOR) members of the heme-copper oxidoreductase (HCO) enzyme superfamily. We identified several previously uncharacterized HCO families, four of which (eNOR, sNOR, gNOR, and nNOR) appear to perform NO reduction. These families have novel active-site structures and several have conserved proton channels, suggesting that they might be able to couple NO reduction to energy conservation. We isolated and biochemically characterized a member of the eNOR family from the bacterium *Rhodothermus marinus* and found that it performs NO reduction. These recently identified NORs exhibited broad phylogenetic and environmental distributions, greatly expanding the diversity of microbes in nature capable of NO reduction. Phylogenetic analyses further demonstrated that NORs evolved multiple times independently from oxygen reductases, supporting the view that complete denitrification evolved after aerobic respiration.

denitrification | heme-copper oxygen reductase | nitric oxide reductase | *Rhodothermus marinus* | aerobic denitrification

Significance

With the advent of culture-independent techniques for studying environmental microbes, our knowledge of their diversity has exploded, uncovering unique organisms, pathways, and proteins carrying out important processes in the biosphere. Novel biochemical reactions are often proposed based on sequence data, but experimental validation is difficult and rare. In this work, we used environmental sequence data to find enzymes that produce the greenhouse gas N_2O from NO and validated our hypothesis with experiments. These new enzymes likely contribute to global N_2O fluxes and expand the breadth of nitrogen cycling. We also demonstrated that these enzymes evolved multiple times from oxygen reductases, indicating that the evolutionary histories of aerobic respiration and denitrification—and more broadly the oxygen and nitrogen cycles—are tightly connected.

The heme-copper oxidoreductase (HCO) superfamily is extremely diverse, with members playing crucial biogeochemical roles in both aerobic (oxygen reductases) and anaerobic [nitric oxide reductases (NORs)] respiration (1–3). While NO reduction can also be performed by fungal NORs (4) and flavodiiron proteins (5), in this paper we focus on NORs from the HCO superfamily. Fungal NO reduction is performed by cytochrome P450 (6), and flavodiiron proteins are primarily used for detoxification of NO. Respiratory denitrification in both Bacteria and Archaea involves NORs from the HCO superfamily. The HCO superfamily consists of three well-characterized oxygen reductase families (A, B, and C) and three NOR families (cNOR, qNOR, and qCu_ANOR) (1–3). The oxygen reductases catalyze the reduction of O_2 to water ($O_2 + 4e^-_{out} + 4H^+_{in} + nH^+_{in} \rightarrow 2H_2O + nH^+_{out}$) and share a conserved reaction mechanism (3, 7), wherein three of the electrons required to reduce O_2 are provided by the active-site metals, heme-Fe and Cu_B, while the fourth electron is derived from a unique redox-active cross-linked histidine-tyrosine cofactor (8) (Fig. 1). The free energy available from this reaction is converted into a transmembrane proton electrochemical gradient, allowing microbes to harness energy from aerobic respiration. The generation of electrochemical gradient occurs via two different mechanisms: charge separation across the membrane and proton pumping (9, 10). Both the protons used for chemistry (i.e., O_2 reduction to water) and those separately pumped protons are taken up from the electrochemically negative side of the membrane (bacterial cytoplasm) by conserved proton-conducting channels that are composed of conserved polar residues and internal water molecules. The different oxygen reductase families exhibit differential proton pumping stoichiometries ($n = 4$ for the A-family, and $n = 2$ for the B and C-families) (10–12) and thus conserve energy differentially depending on their proton channels—though there is some dispute regarding the proton pumping stoichiometry of the C-family, with some studies reporting $n = 4$ (13). The oxygen reductases also vary in their secondary subunits that function as redox relays from electron donors in the electron transport chain (e.g., cytochrome *c*) to the protein complex active site, with the A and B-families utilizing a Cu_A-containing subunit (14–16) and the C-family containing one or more cytochrome *c* subunits (17) (Fig. 1).

NORs catalyze the reduction of NO to nitrous oxide ($2NO + 2H^+_{out} + 2e^-_{out} + nH^+_{in} \rightarrow N_2O + H_2O + nH^+_{out}$). NO reduction requires 2 molecules of NO to form nitrous oxide. With each N atom decreasing in oxidation state by 1, it is only a 2-electron reaction and does not require the cross-linked histidine-tyrosine cofactor for catalysis

The authors declare no competing interest.

This article is a PNAS Direct Submission. J.J.M. is a guest editor invited by the Editorial Board.

[1]R.M. and J.H. contributed equally to this work.

[2]To whom correspondence may be addressed. Email: ranjani.murali@unlv.edu or james.hemp@meliora.bio.

[3]Present address: School of Life Sciences, University of Nevada, Las VegasLas Vegas, NV 89154.

This article contains supporting information online at https://www.pnas.org/lookup/suppl/doi:10.1073/pnas.2316422121/-/DCSupplemental.

Published June 20, 2024.

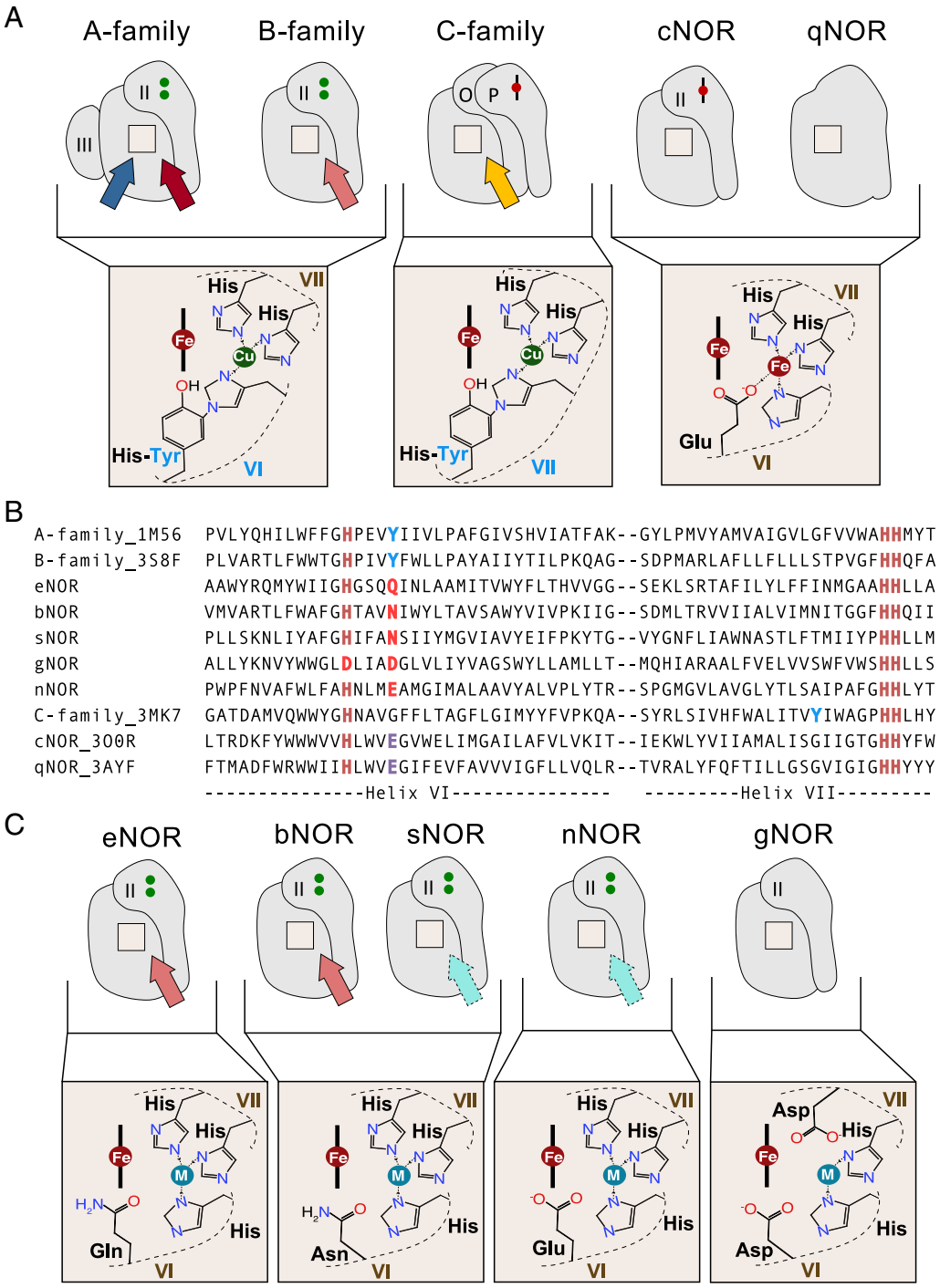

Fig. 1. Comparison of HCO active sites. (*A*) Active-site and proton channel properties of the five characterized HCO families (A-family, B-family, C-family, cNOR, and qNOR). The oxygen reductases all have an active site composed of a high-spin heme, a redox-active cross-linked tyrosine cofactor, and a copper (Cu_B) ligated by three histidines. The A-family has two conserved proton channels, whereas the B- and C-families only have one. The active sites of the NORs are composed of a high-spin heme and an iron (Fe_B) that is ligated by three histidines and a glutamate. Notably, they are missing the tyrosine cofactor. The cNOR and qNOR are also missing conserved proton channels. (*B*) Sequence alignment of the active sites of the recently found HCO families that are related to the B-family. (*C*) Predicted active sites and proton channels for the recently identified HCO families. The eNOR, bNOR, sNOR, and nNOR families contain completely conserved proton channels shown here as arrows. The putative proton channel in the bNOR and eNOR families are highly similar to the K-channel from the B-family oxygen reductase and are colored in red. The K-channel in the B-family is also similar to the K-channel in the A-family oxygen reductase which is colored in dark red. The proton channel in the C-family is different from these channels and is marked in yellow. The putative proton channels in sNOR and nNOR are marked in cyan and differentiated from the other channels with a dashed black outline.

(18)—providing one metric for identifying putative NORs from environmental sequence data. There are currently three biochemically characterized NORs within the HCO superfamily, the cNOR, qNOR, and qCu_ANOR. The cNOR and qNOR families have a four amino acid coordinated Fe_B ion in their active sites, in contrast to the three amino acid coordinated Cu_B found in the HCO oxygen reductases (18–20). The cNOR and qNOR families are closely related to the C-family oxygen reductases (21). Like the C-family O_2 reductase, cNOR has a secondary cytochrome *c* subunit, while qNOR appears to be the result of

a gene fusion of the primary and secondary subunits forming a single polypeptide that lacks the heme *c* binding motif (22–24). cNOR does not conserve energy, with the enzyme taking both electrons and protons for NO reduction from the periplasmic side (25). Although qNOR is proposed to take up protons from the cytoplasm for NO reduction (20, 26), it does not have conserved residues that could form a proton channel from the cytoplasm, and it is not clear whether this enzyme conserves energy via either charge separation or proton pumping. The qCu_ANOR from *Bacillus azotoformans* (2, 27) is not closely related to cNOR and qNOR and is instead derived from within the B-family O_2 reductases, leading it to be reclassified as the bNOR family (23). bNOR is fundamentally different from cNOR and qNOR, containing a Cu_A cofactor in the secondary subunit and a conserved proton channel for proton uptake from the cytoplasm. bNOR was shown to be electrogenic (27) and thus capable of generating more energy than previously characterized NORs. In earlier work, Hemp and Gennis demonstrated that the HCO superfamily was more diverse than previously thought, working with data from archaeal genomes (1). With recent work in a larger dataset including Bacteria and Archaea, we expanded that diversity to 12 families and demonstrated that quinol oxidation evolved within the HCO superfamily multiple times (23). In this work, we used phylogenomics of both isolates and environmental sequence data to study the diversity and evolution of multiple putative NOR families (eNOR, gNOR, nNOR, and sNOR) within the HCO superfamily and verified the biochemical NO reduction activity of eNOR from the bacterium, *Rhodothermus marinus*. We also identified a new family of putative N_2O reductases. Our findings expanded the number of denitrification pathways in Bacteria and Archaea, increased the breadth of modern N_2O production and further constrained the evolutionary history of one of the key protein scaffolds involved in aerobic and anaerobic respiration.

Results and Discussion

Expansion of the HCO Superfamily. Phylogenomic analyses of genomic and metagenomic data identified at least six new families belonging to the HCO superfamily (Figs. 1 and 2) that are missing the active-site tyrosine, indicating that they do not catalyze O_2 reduction. Analysis of structural models and sequences (*SI Appendix*) for each of these families showed no evidence for the sequence migration of a conserved tyrosine that could form an active-site cross-linked cofactor, as was observed in the C-family O_2 reductases (8). Furthermore, their active sites exhibited structural features never before seen within the superfamily (Fig. 1). One of these families is closely related to qNOR and has been proposed to be a NO dismutase (NOD) contributing to intracellular O_2 production in "*Candidatus* Methylomirabilis oxyfera" (28, 29). Another family is closely related to cNOR and might serve as a unique sulfide and acetylene-insensitive nitrous oxide reductase (N_2O red) (30, 31). The remaining four families (eNOR, sNOR, nNOR, and gNOR) are closely related to the B-family of O_2 reductases (Fig. 2) and encode homologs of the Cu_A-containing secondary subunits. This is consistent with the presence of Cu_A-containing subunits in the B-family of oxygen reductases (Fig. 1 and Dataset S1). Based on modeled active-site structures and genomic context, we proposed that these novel families perform NO reduction (Fig. 1).

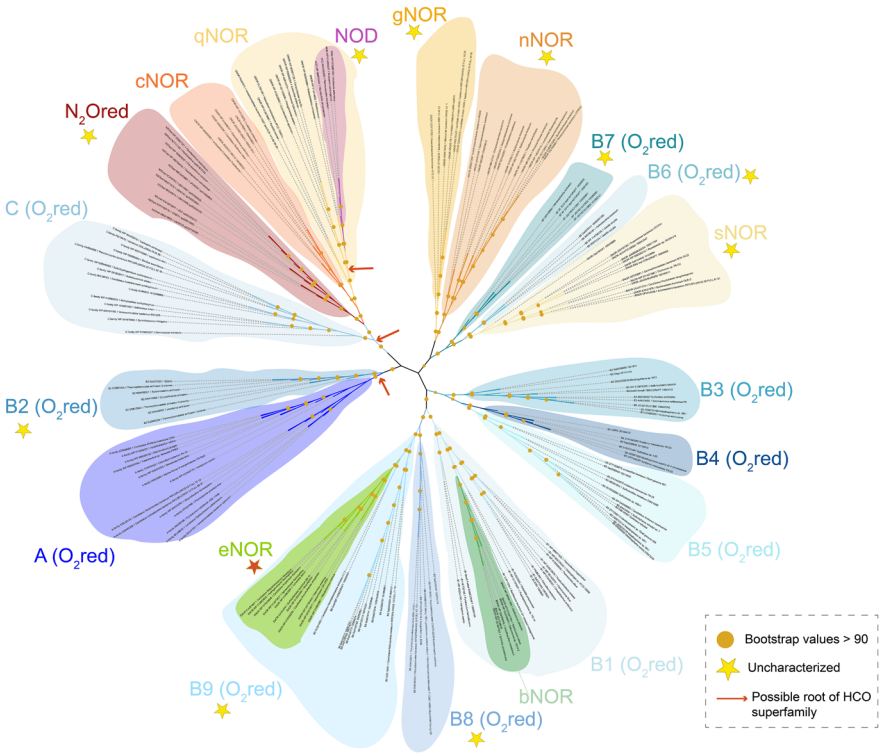

Fig. 2. Evolution of NORs. An unrooted phylogenetic tree of HCO sequences was inferred from a multiple sequence alignment (Dataset S2—Multiple sequence alignment) of a representative set of HCO sequences using IQ-Tree as described in *Materials and Methods*. Each of the HCO families is shaded in a different color. Oxygen reductases are in shades of blue, whereas NORs are in shades of yellow, green, and red. The putative N_2O red family is depicted in a light shade of red. The eNOR, bNOR, nNOR, gNOR and sNOR families are derived from oxygen reductase ancestors. Putative root positions (within the A-family, in the qNOR or between the A- and C-families) for the HCO superfamily are noted with a red arrow based on previous literature (32, 33). Uncharacterized enzymes are indicated with a yellow star while the eNOR is indicated with a red star. The Newick tree file is available as Dataset S3 and a list of the leaf labels is available as Dataset S4.

Biochemical Characterization of eNOR. To validate these predictions, we isolated and biochemically characterized a member of the eNOR family from *R. marinus* DSM 4252, a thermophilic member of the Bacteroidetes phylum. *R. marinus* was originally classified as a strict aerobe (34), but its genome encoded a periplasmic nitrate reductase (NapA), two nitrite reductases (NirS and NirK), and a N_2O reductase (NosZ), suggesting that it may also be capable of denitrification (*SI Appendix*, Fig. S1). Denitrification was not observed under strictly anaerobic conditions, however, under microoxic conditions, we observed that isotopically labeled $^{15}NO_3^-$ was converted to $^{30}N_2$ (*SI Appendix*, Fig. S2), demonstrating that *R. marinus* DSM 4252 was capable of complete aerobic denitrification ($NO_3^-\rightarrow N_2$). Blockage of the N_2O red (NosZ) with acetylene led to the accumulation of N_2O (Fig. 3), implying that a NOR was also present in *R. marinus* DSM 4252. No known NORs (cNOR, qNOR, qCu_ANOR/bNOR, or flavodiiron proteins) were found in the genome. However, *R. marinus* DSM 4252 encoded a member of the eNOR family (*SI Appendix*, Fig. S1).

Isolation and biochemical characterization of the *R. marinus* DSM 4252 eNOR protein verified that it catalyzed NO reduction [at 25 °C, k_{cat} = 0.68 ± 0.21 NO s^{-1} (n = 4)] (Fig. 3). This turnover number is lower than catalytic turnover rates reported for NORs purified from mesophilic bacteria such as *Pseudmonas stutzeri* [16 NO s^-] (35) or *Neisseria meningitidis* [30 NO s^-] (20) but is higher than activities reported for cNOR purified from other thermophilic microorganisms such as *Thermus thermophilus* [0.09 NO s^-] (25). eNOR was unable to catalyze O_2 reduction using a range of electron donors (*SI Appendix*, Fig. S3), showing that it functioned solely as a NOR. UV–Vis spectroscopy and heme characterization via mass spectrometry demonstrated that the *R. marinus* DSM 4252 eNOR contained a unique modified heme *a* that is used in both heme sites (Fig. 3 and *SI Appendix*, Figs. S3 and S4). Another member of the eNOR family was previously isolated from the aerobic denitrifier *Magnetospirillum magnetotacticum* MS-1 (36, 37); however, its function was never determined. The UV–Vis spectra of the *M. magnetotacticum* eNOR (36) were identical to the *R. marinus* eNOR, implying that the modified heme *a* is a general feature of the family. Mass spectroscopic analysis of the hemes extracted from eNOR revealed that this heme was A_s—a previously isolated heme *a* with a hydroxyethylgeranylgeranyl side chain first identified in the B-family oxygen reductase from *Sulfolobus acidocaldarius* (38). Many eNOR operons contain a CtaA homolog, an O_2-dependent enzyme that converts heme *o* to heme *a* (39). This is consistent with the observation that eNOR required microoxic conditions to be expressed. Organisms performing denitrification with eNOR appear to be obligate aerobic denitrifiers, and future work will establish the extent of their role in environmental aerobic denitrification (40).

Unique Active-Site Features of recentiy identified NORs. In addition to the experimental evidence that both eNOR and bNOR enzymes are NO reductases, there are several reasons to predict that the other recently identified families also perform NO reduction. The sNOR family has the same active-site structure as the bNOR family, strongly suggesting that it also performs NO reduction. However, the sNOR and bNOR families are not closely

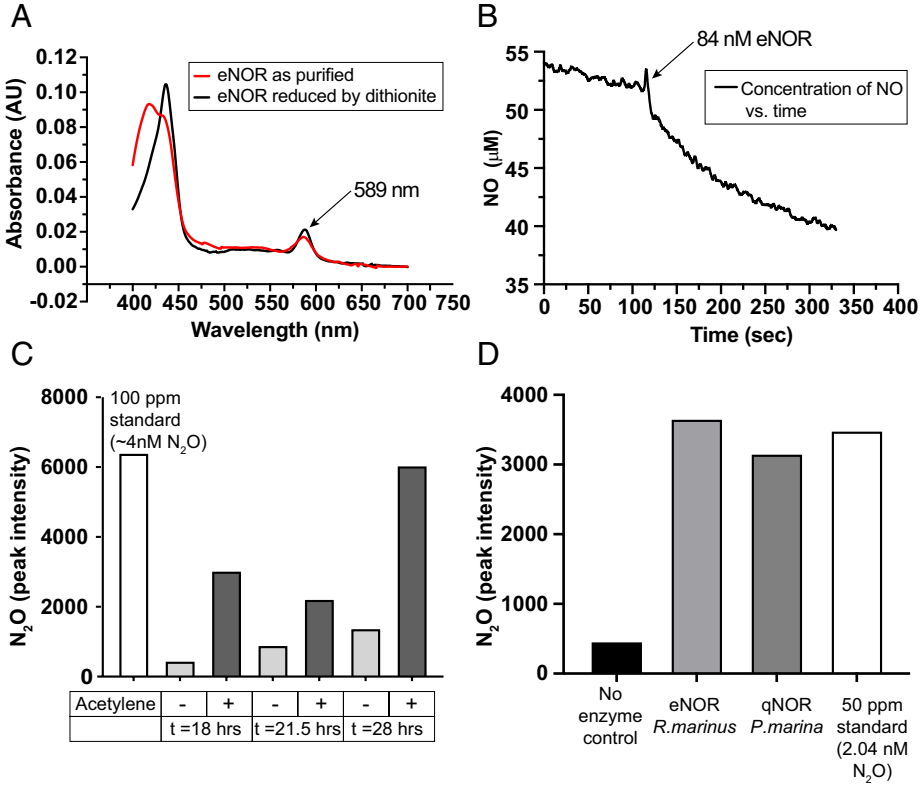

Fig. 3. Biochemical Characterization of the eNOR from *R. marinus*. (*A*) UV–Visible spectrum of isolated eNOR indicated the presence of an unusual heme *a* signature at 589 nm. (*B*) NO reductase activity was measured with the use of a Clark electrode in the presence of N, N, N′, N′-tetramethyl-p-phenylenediamine (TMPD) and ascorbate as electron donor. (*C*) N_2O accumulation was observed in an actively growing culture of *R. marinus*. Then, 5 mL was subsampled from a 1 L culture of *R. marinus* and incubated at 42 °C for 30 min in an anaerobic stoppered serum vial with or without acetylene, an inhibitor of the terminal enzyme in denitrification, N_2O red or NosZ. The headspace gas from this incubation was sampled and N_2O concentrations were measured with gas chromatography (GC) followed by analysis by an electron capture detector (ECD). (*D*) N_2O production by eNOR from *R. marinus* and qNOR from *Persephonella marina* were measured using GC-ECD following incubation of the pure enzyme with TMPD, Ascorbate, and NO under the same conditions as described for subsamples of the culture in *C*.

related and mark an example of convergent evolution of active-site structures within the HCO superfamily (Figs. 1 and 2). We identified another example of convergent evolution in the nNOR family. Members of this family have the same conserved active-site residues as the cNOR and qNOR families (Fig. 1) but are only very distantly related to them; nNOR is related to the B-family, whereas cNOR and qNOR are related to the C-family. Interestingly, the low-spin heme in nNOR is ligated by a histidine and methionine, which likely raises its redox potential by ~150 mV (41). This feature is similar to a modification found in some eNORs, wherein the low-spin heme is ligated by histidine and lysine. The gNOR is the first example of a HCO family member that has replaced one of the active-site histidines—residues completely conserved in all other families. The gNOR active site, with an aspartate in place of histidine, is likely capable of catalyzing NO reduction, since NO reduction was demonstrated in a bioinorganic mimic of the gNOR active-site (42). The gNOR has a secondary subunit with a cupredoxin fold that is missing the residues required to bind Cu_A, similar to the quinol-oxidizing oxygen reductase cytochrome bo_3 from *Escherichia coli*. Conserved residues that could bind quinol have been identified in gNOR, so it may be a quinol-oxidizing NOR similar to qNOR (23).

The biochemically characterized eNOR and bNOR and proposed sNOR and gNOR families within the HCO superfamily have active sites that differ significantly from those found in the well-characterized cNOR and qNOR enzymes (Fig. 1). Importantly, while oxygen reduction chemistry is constrained to require a redox-active tyrosine cofactor, multiple HCO active-site structures appear to be compatible with NO reduction chemistry. Oxygen reductases from the A-family, B-family, and C-family (18, 43, 44) appear to catalyze NO reduction, albeit less efficiently and with a different mechanism than the NORs. This difference in biochemical constraints between NO and oxygen reduction chemistry suggests that the evolutionary transition of oxygen reduction to NO reduction is relatively simple within the HCO superfamily. Another useful chemical constraint that appears to differentiate the catalysis of O_2 reduction and NO reduction is the active site metal: in the currently characterized HCOs, Cu_B is utilized for O_2 reduction chemistry, whereas Fe_B is used for NO reduction chemistry. If this pattern is verified for the other predicted NOR families, it would indicate that the chemistry performed by HCOs is determined to a certain degree by the electronic properties of the active-site metal. It is important to note that the above biochemical constraints for NO and O_2 reduction chemistry are only applicable within the HCO superfamily, since other enzymes such as the flavodiiron proteins (5) or cytochrome *bd* oxygen reductases (45) are capable of NO and O_2 reduction with entirely different active site characteristics. Interestingly, tryptophan/tyrosine chains that are predicted to prevent oxidative damage in redox-active proteins (46) are conserved in both the A-family and B-family O_2 reductases and several of the NO reductases that have evolved from the B-family (bNOR, eNOR, and gNOR) (Dataset S5). In these chains, radicals generated during substrate turnover move by hole hopping through a series of tryptophan and tyrosine residues to the surface of the protein where they are safely quenched by redox buffers within the cell (e.g., glutathione). Despite the difference in catalytic mechanisms between O_2 reductases, 2 out of 3 residues implicated in oxidative protection are found in bNOR, eNOR, and gNOR; they are missing in sNOR and nNOR. Future investigation of the catalytic differences between these NORs will provide insight into the role played by these residues.

Bioenergetics of Denitrification Pathways with Recently Identified NORs. Although both denitrification and aerobic respiration are highly exergonic processes, most of the enzymes in the denitrification pathway are not directly coupled to energy conservation in cells, making denitrification less energetically efficient than aerobic respiration (47). In the HCO oxygen reductases, conserved proton channels deliver protons from the cytoplasm to the active site for chemistry. These same channels are used to pump protons to the periplasmic side (9, 11, 12, 48). In contrast, previously characterized NORs do not appear to pump protons or conserve as much energy as the oxygen reductases. cNOR does not have conserved proton channels from the cytoplasm, which makes this enzyme incapable of conserving energy (25). The evidence regarding qNOR is currently ambiguous: although qNOR does not have conserved proton channels either, there is some evidence suggesting that it can conserve energy (20, 26).

We found that eNOR family has conserved hydrophilic residues, similar to the electrogenic bNOR, that closely resemble those found in the proton-conducting K-channel within the B-family of oxygen reductases (12, 27) (Dataset S1 and *SI Appendix*, Fig. S5). The sNOR family also has conserved residues in the K-channel region. However, this putative proton channel is slightly different from those found in the B1-subfamily of O_2 reductases (that contains the *T. thermophilus* ba_3) and the eNOR and bNOR families (Dataset S1). The conserved serine (S309, B1-subfamily *T. thermophilus* ba_3 numbering) found in those families is missing in the sNOR, and instead, this enzyme has a conserved glutamate residue in a structurally different location from other HCO enzymes. Interestingly, the nNOR family, which has the same active site as cNOR and qNOR, also has a conserved proton channel (Dataset S1 and *SI Appendix*, Fig. S5). This implies that these recently identified NORs may be capable of energy conservation and the lack of a proton channel in the cNOR and qNOR may not be due to energetic constraints universal to NO reduction (49). The conserved proton channels in the eNOR, bNOR, sNOR, and nNOR families would allow them to conserve energy via charge separation and potentially by proton pumping. Detailed characterization of these new NOR families will be helpful for understanding the mechanism of proton pumping in the HCO superfamily—one of the long-standing questions in bioenergetics (50).

Environmental Distribution of NORs. The recently identified HCO NOR families have broad phylogenetic and environmental distributions that substantially expand the scope of denitrification occurring in nature (Table 1 and Datasets S6 and S7). The eNOR, sNOR, gNOR, and nNOR families are all found in both Bacteria and Archaea, whereas the bNOR family was only found in the Bacillales order of Firmicutes (Dataset S6). Phylogenetic analysis of metagenomic data shows that the majority of eNOR, sNOR, gNOR, and nNOR enzymes appear in uncharacterized taxa, hinting at many more organisms capable of NO reduction than previously suspected. Furthermore, the new HCO NOR families were found in a wide variety of environments (Table 1 and Dataset S7). sNORs are broadly distributed in many environments, however, they are rarely found in Archaea. sNORs are found in most ammonia-oxidizing bacteria (AOB) sequenced to date, suggesting that the capability of NO reduction is an important difference in ammonia oxidation pathways between Bacteria and Archaea. Given the importance of AOB, it is likely that sNOR plays a role in this key biogeochemical process in nature (Dataset S7). The gNORs were predominantly found in microbes inhabiting sulfidic environments and as mentioned above may reflect an adaptation that allows for denitrification in the presence of free sulfide, which inhibits other NOR families (Dataset S7). Our analyses revealed that the eNOR family—the new HCO enzyme characterized in detail here—is extremely common in nature and has a broad distribution, similar to the cNOR and qNOR families (Datasets S6 and S7).

Table 1. Distribution of families from the HCO superfamily in various public databases

	NCBI-Genomes	IMG-metagenomes	GTDB-genomes
A-family	20,290	102,368	45,135
B-family	1,238	4,683	2,021
C-family	13,976	23,015	14,981
qNOR	4,388	7,680	3,458
cNOR	2,801	4,824	2,594
eNOR	68	2,709	547
sNOR	95	872	344
bNOR	51	12	200
nNOR	6	289	32
gNOR	10	913	156
NOD	8	539	108
N_2O red	25	597	293

Distribution of NOR families in sequenced genomes vs. environmental datasets. The recently found NOR families account for approximately 2/3 of currently known diversity and 1/2 of the abundance of NORs in nature.

eNORs were found in many strains of *Candidatus* Accumulibacter phosphatis, a critical microbe utilized in wastewater treatment plants for enhanced biological phosphorus removal. The eNOR is highly expressed in transcriptomic datasets from these facilities, demonstrating that *Ca.* Accumulibacter phosphatis is capable of complete denitrification in situ (51). eNOR has also been found in microbes capable of performing autotrophic nitrate reduction coupled to Fe(II) oxidation (NRFO). *Gallionellaceae* KS and related strains express an eNOR under denitrifying conditions, suggesting that an individual organism is capable of complete NRFO (52). eNOR is also common in hypersaline environments (Dataset S7), where it might play a role in the adaptation of denitrification to high salt conditions.

Many organisms encode NORs from multiple families (e.g., *Candidatus* Methylomirabilis oxyfera has qNOR, sNOR, and gNOR; *B. azotoformans* has qNOR, sNOR, and bNOR). The reasons underlying this apparent redundancy remain unclear, but it suggests that selection for different enzymatic properties (NO affinity, enzyme kinetics, energy conservation, or sensitivity to inhibitors) or the concentration of O_2 may be important factors in determining their distribution and use, similar to what was observed for the HCO oxygen reductase families (10). Analysis of the presence of denitrification genes (nitrite reductases, NORs, and the NosZ-type N_2O reds) within sequenced genomes revealed that many more organisms are capable of complete denitrification than previously realized (Dataset S8). Our current understanding of the diversity of organisms capable of performing denitrification in nature is far from complete but stands to grow with the recognition of these new families of NORs.

The Intertwined Evolutionary History of Aerobic Respiration and Denitrification. Combining our biochemical results and insights with the phylogenetic relationships among different groups in the HCO superfamily, which contains both oxygen reductases and NORs, allowed us to better ordinate the evolutionary histories of aerobic respiration and denitrification. Previous work had demonstrated close evolutionary relationships between the A and B-family oxygen reductases (3), as well as close ancestry between the C-family oxygen reductases, cNOR, and qNOR (21). Yet, the question of which arose first—denitrification or aerobic respiration—has been harder to resolve.

Our analysis of the distribution of oxygen reductases and NORs across the wide diversity of microbial life revealed that oxygen reductases are far more widely distributed; over 30,238 of the 47,894 species in the genome taxonomy database (GTDB) encoded oxygen reductases, whereas NORs were only found in 6,626 species (Datasets S6 and S8). This distribution illustrated the massive impact that oxygen has had on the energetics of the biosphere. The A-family is by far the most widely distributed of the HCO enzymes. It is found in all three domains of life and in more phyla than any other enzyme of the HCO superfamily. This is consistent with the view that the A-family oxygen reductase holds greater antiquity (1, 10, 32, 53), wherein the B-family and C-family O_2 reductases each evolved independently from within the A-family to facilitate specific metabolic and ecological challenges associated with exotic flavors of aerobic biology, like in hyperthermophiles (15) or in chemoautotrophic iron oxidation (54). An evolutionary transition from the A-family to B-family due to selection for higher oxygen affinity, which led to the loss of the D-proton channel to facilitate greater access of oxygen to the active site has been inferred from structural and phylogenetic data with a putative intermediate enzyme suggested in *Nitrosopumilis maritimus* (10). With that in mind, a clear transition from A to the C-family oxygen reductases has not been demonstrated.

The C-family branch of the HCO superfamily consists of the closely related C-family oxygen reductase, N_2O red, cNOR, qNOR, and NOD (Fig. 2) (3, 21, 29, 33, 55). The transition from cNOR to qNOR as the result of a gene fusion of subunits I and II has been reasonably inferred based on the sequence similarity between the N-terminal domain of qNOR and subunit II of cNOR (24). That NOD was derived from qNOR is supported by the high level of sequence similarity between qNOR and NOD, as well as its branching topology within the qNOR clade (Fig. 2). These relative constraints support a simple interpretation of the evolutionary history within this branch—the C-family is the oldest, followed by the evolution of the N_2O red and cNOR. The cNOR then is the ancestor of qNOR, followed by NOD. The sparse distribution of the C-family oxygen reductases, cNOR, and NOD in Archaea supports the hypothesis that these families evolved after the A-family oxygen reductases. While qNOR is widely distributed, it is rarely associated with energetically efficient denitrification and has been proposed to function in nature as a detoxification enzyme (21). Therefore, the presence of qNOR cannot be used as a robust constraint for the antiquity of denitrification. The wide distribution of the A-family, the indications of an evolutionary transition from the A- to B-family, and the relatively sparse distribution of the C-family branch members in Archaea, all suggest that the A-family likely hosts the root of the HCO superfamily (Fig. 2). In the future, the use of different comparative biological approaches—particularly those that might better capture the evolution of paralogs—to root the phylogenetic tree of HCOs could be used to test this idea.

What is clear from our new observations—regardless of the placement of the root of the HCO superfamily—is that NORs have evolved independently multiple times from the B-family and C-family oxygen reductases (Fig. 2). There are key underlying factors that enabled this, both chemical and environmental. It is biochemically straightforward to adapt an oxygen reductase (4 e^- chemistry) for NO reduction (2 e^- chemistry). B and C-family oxygen reductases can reduce NO at high concentrations in vitro (43, 56). It is thus unsurprising that small evolutionary modifications would lead to a cascade of enzyme descendants each capable of NO reduction at lower concentrations to enable more effective denitrification. It is also clear that in many environments, denitrification

and aerobic respiration often co-occur (57, 58), and that many microorganisms display the respiratory flexibility to shift from aerobic to anaerobic respiration, especially at lower O_2 concentrations (59). This respiratory flexibility is reflected in the fact that denitrification and oxygen respiration share much of the same bioenergetic logic, conserving energy via complex III or alternative complex III (60). Thus, the biochemical promiscuity of O_2 reductases toward NO, the ecological proximity of NO_3^- and O_2, and the close similarity between their respiratory pathways help explain why the evolutionary transition of O_2 reduction to NO reduction is both favorable and readily achievable.

Nitrate is derived from biogeochemical processes involving oxygen (61) and consequently opportunities for denitrification prior to Earth's great oxygenation event (GOE) were muted compared to those after the GOE with the rise of nitrate in seawater. Finally, both aerobic respiration and denitrification are constrained by the presence of copper. Copper is an essential bioinorganic component of the active site in the O_2 reductases, nitrite reductase NirK, and for N_2O red (NosZ) and is therefore essential for their biochemical activity. The environmental abundance of copper increased significantly after the GOE (62–64), suggesting that both of these metabolic pathways evolved and expanded after the accumulation of O_2 in Earth's surface environments.

Materials and Methods

This is an abbreviated version of the materials and methods used in this work. A detailed version is available as part of *SI Appendix*.

Purification of eNOR from *R. marinus* Grown under Denitrification Conditions. *R. marinus* DSMZ 4252 was grown in DSM Medium 630 with 30 mM NO_3^- added and shaken at 75 rpm to induce denitrification. The microoxic conditions that result from slow shaking were essential for denitrification in *R. marinus*. We used labeled nitrate ($^{15}NO_3^-$) to verify that *R. marinus* DSM 4252 was capable of complete denitrification (NO_3^- to N_2). The experiments detailed below established that eNOR was expressed under these conditions and functions as a NOR.

Cultures of *R. marinus* were grown in 1L of this medium in 24 × 2L Erlenmeyer flasks for 36 h or to stationary phase, to generate sufficient biomass for protein purification. The cell pellet recovered from this culture was subject to lysis as described in *SI Appendix, Materials and Methods* and the membrane fraction was recovered by ultracentrifugation. eNOR was purified in a protocol similar to that described for caa_3 from *R. marinus* (65). Purification of eNOR was improved when the membranes were first solubilized in 1% 3-[(3-Cholamidopropyl) dimethylammonio]-1-propanesulfonate (CHAPS), apparently recovering peripheral membrane proteins. The membranes not solubilized in this step were then pelleted with ultracentrifugation and solubilized in 1% N-dodecyl-β-D-maltoside (DDM). These solubilized membrane proteins were subject to a protein purification protocol detailed in *SI Appendix, Materials and Methods*. Purified protein was confirmed to be eNOR using electrophoretic analysis and mass spectrometric identification.

Biochemical Characterization of eNOR. Purified eNOR was verified to perform NO reduction by measuring NO consumption using a Clark Electrode (World Precision Instruments) in a protocol previously described (25) and by measurement of the product, N_2O using GC.

The heme cofactors of eNOR were first analyzed using a pyridine hemochrome assay (66) and then analyzed by Liquid Chromatography-Mass Spectrometry (LC-MS) after solvent extraction. Further details for both assessment of activity and cofactor identification are available in *SI Appendix, Materials and Methods*.

A detailed description of the phylogenomic analysis of NORs by taxonomy and environment is provided in *SI Appendix, Materials and Methods*.

Data, Materials, and Software Availability. All the protein accession numbers used for generation of trees in this study, as well as associated phylogenetic trees and multiple sequence alignments are included in the supporting information. The Hidden Markov Models (HMMs) used for identification of HCO sequences can be found at https://github.com/ranjani-m/HCO (67).

ACKNOWLEDGMENTS. We thank the NIH for funding support (grant# U12AB123456 to PI: R.B.G.). This research was also supported by funding from the Agouron Institute (W.W.F. and J.H.) and by the Community Science Project 507064 (PI: R.H.) under the Joint Genome Institute (https://ror.org/04xm1d337), which is a Department of Energy (DOE) Office of Science User Facility. Resources were also used at Office of Biological and Environmental Research of the US Department of Energy Atmospheric System Research Program Interagency Agreement grant DE-AC02-05CH11231 (JGI). Resources were used at Office of Biological and Environmental Research of the United States Department of Energy Atmospheric System Research Program Interagency Agreement grant DE-AC05-76RL01830 Environmental Molecular Sciences Laboratory (EMSL). We thank Sylvia Choi for providing pure ba_3 oxygen reductase from *T. thermophilus* to use as a control for oxygen reductase assays and for heme extraction, Paige Sheridan for providing purified qNOR from *Persephonella marina*, Lici Schurig-Briccio for guidance in performing NOR assays with the Clark Electrode, and Peter Yau at the University of Illinois' Mass spectrometric facility for protein identification. We thank Alon Philosof and Connor Skennerton for valuable discussions on bioinformatics analysis. Finally, we would like to thank our reviewers for their valuable comments that led to the improvement of this manuscript.

Author affiliations: [a]Department of Biochemistry, University of Illinois, Urbana-Champaign, Urbana, IL 61801; [b]Division of Biology and Biological Engineering, California Institute of Technology, Pasadena, CA 91125; [c]School of Life Sciences, University of Nevada, Las Vegas, Las Vegas, NV 89154; [d]meliora.bio, Salt Lake City, UT 84103; [e]Department of Earth Science and Environmental Change, University of Illinois at Urbana-Champaign, Urbana, IL 61801; [f]Department of Geosciences, Smith College, Northampton, MA 01063; [g]Division of Geological and Planetary Sciences, California Institute of Technology, Pasadena, CA 91125; [h]Department of Chemistry and Biochemistry, Thermal Biology Institute, Montana State University, Bozeman, MT 59717; [i]Center for Biofilm Enginering, Montana State University, Bozeman, MT 59717; [j]Department of Microbiology and Cell Biology, Montana State University, Bozeman, MT 59717; and [k]Department of Plant and Microbial Biology, University of California, Berkeley, CA 94720

Author contributions: R.M., W.W.F., R.B.G., and J.H. designed research; R.M., L.A.P., R.A.S., L.M.W., M.M.L., R.H., W.W.F., and J.H. performed research; R.M., R.A.S., L.M.W., W.W.F., R.B.G., and J.H. contributed new reagents/analytic tools; R.M., L.A.P., U.F.L., W.W.F., R.B.G., and J.H. analyzed data; and R.M., R.A.S., L.M.W., M.M.L., R.H., W.W.F., R.B.G., and J.H. wrote the paper.

1. J. Hemp, R. B. Gennis, Diversity of the heme-copper superfamily in archaea: Insights from genomics and structural modeling. *Results Probl. Cell Differ.* **45**, 1–31 (2008).
2. Suharti, M. J. F. Strampraad, I. Schröder, S. de Vries, A novel copper A containing menaquinol NO reductase from Bacillus azotoformans. *Biochemistry* **40**, 2632–2639 (2001).
3. M. M. Pereira, F. L. Sousa, A. F. Veríssimo, M. Teixeira, Looking for the minimum common denominator in haem–copper oxygen reductases: Towards a unified catalytic mechanism. *Biochim. Biophys. Acta* **1777**, 929–934 (2008).
4. K. Maeda *et al.*, N_2O production, a widespread trait in fungi. *Sci. Rep.* **5**, 9697 (2015).
5. C. V. Romão, J. B. Vicente, P. T. Borges, C. Frazão, M. Teixeira, The dual function of flavodiiron proteins: Oxygen and/or nitric oxide reductases. *J. Biol. Inorg. Chem.* **21**, 39–52 (2016).
6. N. Takaya, H. Shoun, Nitric oxide reduction, the last step in denitrification by Fusarium oxysporum, is obligatorily mediated by cytochrome P450nor. *Mol. Gen. Genet.* **263**, 342–348 (2000).
7. J. Hemp, C. Christian, B. Barquera, R. B. Gennis, T. J. Martínez, Helix switching of a key active-site residue in the cytochrome cbb3 oxidases. *Biochemistry* **44**, 10766–10775 (2005).
8. J. Hemp, D. E. Robinson, T. J. Martinez, N. L. Kelleher, R. B. Gennis, The evolutionary migration of a post-translationally modified active-site residue in the proton-pumping heme-copper oxygen reductases. *Biochemistry* **45**, 15405–15410 (2006).
9. M. K. F. Wikstrom, Proton pump coupled to cytochrome c oxidase in mitochondria. *Nature* **266**, 271–273 (1977).
10. H. Han *et al.*, Adaptation of aerobic respiration to low O_2 environments. *Proc. Natl. Acad. Sci. U.S.A.* **108**, 14109–14114 (2011).
11. J. Hemp *et al.*, Comparative genomics and site-directed mutagenesis support the existence of only one input channel for protons in the C-family (cbb3 oxidase) of heme-copper oxygen reductases. *Biochemistry* **46**, 9963–9972 (2007).
12. H.-Y. Chang *et al.*, Exploring the proton pump and exit pathway for pumped protons in cytochrome ba3 from Thermus thermophilus. *Proc. Natl. Acad. Sci. U.S.A.* **109**, 5259–5264 (2012).
13. V. Rauhamäki, D. A. Bloch, M. Wikström, Mechanistic stoichiometry of proton translocation by cytochrome cbb3. *Proc. Natl. Acad. Sci. U.S.A.* **109**, 7286–7291 (2012).

14. L. Qin, C. Hiser, A. Mulichak, R. M. Garavito, S. Ferguson-Miller, Identification of conserved lipid/detergent-binding sites in a high-resolution structure of the membrane protein cytochrome c oxidase. *Proc. Natl. Acad. Sci. U.S.A.* **103**, 16117–16122 (2006).
15. T. Soulimane *et al.*, Structure and mechanism of the aberrant ba3-cytochrome c oxidase from Thermus thermophilus. *EMBO J.* **19**, 1766–1776 (2000).
16. T. Tiefenbrunn *et al.*, High resolution structure of the ba3 cytochrome c oxidase from Thermus thermophilus in a lipidic environment. *PLoS One* **6**, 1–12 (2011).
17. S. Buschmann *et al.*, The structure of cbb3 cytochrome oxidase provides insights into proton pumping. *Science* **329**, 327–330 (2010).
18. N. Lehnert *et al.*, The biologically relevant coordination chemistry of iron and nitric oxide: Electronic structure and reactivity. *Chem. Rev.* **121**, 14682–14905 (2021).
19. T. Hino *et al.*, Structural basis of biological N_2O generation by bacterial nitric oxide reductase. *Science* **330**, 1666–1670 (2010).
20. N. Gonska *et al.*, Characterization of the quinol-dependent nitric oxide reductase from the pathogen Neisseria meningitidis, an electrogenic enzyme. *Sci. Rep.* **8**, 3637 (2018).
21. W. G. Zumft, Nitric oxide reductases of prokaryotes with emphasis on the respiratory, heme–copper oxidase type. *J. Inorg. Biochem.* **99**, 194–215 (2005).
22. Y. Matsumoto *et al.*, Crystal structure of quinol-dependent nitric oxide reductase from Geobacillus stearothermophilus. *Nat. Struct. Mol. Biol.* **19**, 238–245 (2012).
23. R. Murali, J. Hemp, R. B. Gennis, Evolution of quinol oxidation within the heme-copper oxidoreductase superfamily. *Biochim. Biophys. Acta* **1863**, 148907 (2022).
24. J. Hendriks *et al.*, Nitric oxide reductases in bacteria. *Biochim. Biophys. Acta* **1459**, 266–273 (2000).
25. L. A. Schurig-Briccio *et al.*, Characterization of the nitric oxide reductase from Thermus thermophilus. *Proc. Natl. Acad. Sci. U.S.A.* **110**, 12613–12618 (2013).
26. C. C. Gopalasingam *et al.*, Dimeric structures of quinol-dependent nitric oxide reductases (qNORs) revealed by cryo–electron microscopy. *Sci. Adv.* **5**, eaax1803 (2019).
27. S. Al-Attar, S. de Vries, An electrogenic nitric oxide reductase. *FEBS Lett.* **589**, 2050–2057 (2015).
28. K. F. Ettwig *et al.*, Nitrite-driven anaerobic methane oxidation by oxygenic bacteria. *Nature* **464**, 543–548 (2010).
29. K. F. Ettwig *et al.*, Bacterial oxygen production in the dark. *Front. Microbiol.* **3**, 273 (2012).
30. A. M. Jones, A. M. Adkins, R. Knowles, G. R. Rayat, Identification of a denitrifying gliding bacterium, isolated from soil and able to reduce nitrous oxide in the presence of sulfide and acetylene, as Flexibacter canadensis. *Can. J. Microbiol.* **36**, 765–770 (1990).
31. A. M. Jones, T. C. Hollocher, R. Knowles, Nitrous oxide reductase of Flexibacter canadensis: A unique membrane-bound enzyme. *FEMS Microbiol. Lett.* **92**, 205–209 (1992).
32. M. M. Pereira, M. Santana, M. Teixeira, A novel scenario for the evolution of haem–copper oxygen reductases. *Biochim. Biophys. Acta* **1505**, 185–208 (2001).
33. A.-L. Ducluzeau *et al.*, The evolution of respiratory O2/NO reductases: An out-of-the-phylogenetic-box perspective. *J. R. Soc. Interface* **11**, 20140196 (2014).
34. G. A. Alfredsson, J. K. Kristjansson, S. Hjrleifsdottir, K. O. Stetter, Rhodothermus marinus, gen. nov., sp. nov., a Thermophilic, Halophilic Bacterium from submarine hot springs in Iceland. *J. Gen. Microbiol.* **134**, 299–306 (1988).
35. B. Heiss, K. Frunzke, W. G. Zumft, Formation of the N-N bond from nitric oxide by a membrane-bound cytochrome bc complex of nitrate-respiring (denitrifying) Pseudomonas stutzeri. *J. Bacteriol.* **171**, 3288–3297 (1989).
36. H. Tamegai, T. Yamanaka, Y. Fukumori, Purification and properties of a 'cytochrome a1'-like hemoprotein from a magnetotactic bacterium, Aquaspirillum magnetotacticum. *Biochim. Biophys. Acta* **1158**, 237–243 (1993).
37. Y. Tanimura, Y. Fukumori, Heme-copper oxidase family structure of Magnetospirillum magnetotacticum 'cytochrome a1'-like hemoprotein without cytochrome c oxidase activity. *J. Inorg. Biochem.* **82**, 73–78 (2000).
38. M. Lübben, K. Morand, Novel prenylated hemes as cofactors of cytochrome oxidases. Archaea have modified hemes A and O. *J. Biol. Chem.* **269**, 21473–21479 (1994).
39. K. R. Brown, B. M. Allan, P. Do, E. L. Hegg, Identification of novel hemes generated by heme A synthase: Evidence for two successive monooxygenase reactions. *Biochemistry* **41**, 10906–10913 (2002).
40. B. Ji *et al.*, Aerobic denitrification: A review of important advances of the last 30 years. *Biotechnol. Bioproc. E* **20**, 643–651 (2015).
41. C. Fufezan, J. Zhang, M. R. Gunner, Ligand preference and orientation in b- and c-type heme-binding proteins. *Proteins* **73**, 690–704 (2008).
42. Y.-W. Lin *et al.*, Introducing a 2-His-1-Glu nonheme iron center into myoglobin confers nitric oxide reductase activity. *J. Am. Chem. Soc.* **132**, 9970–9972 (2010).
43. A. Giuffrè *et al.*, The heme-copper oxidases of Thermus thermophilus catalyze the reduction of nitric oxide: Evolutionary implications. *Proc. Natl. Acad. Sci. U.S.A.* **96**, 14718 (1999).
44. E. Forte *et al.*, The cytochrome cbb3 from Pseudomonas stutzeri displays nitric oxide reductase activity. *Eur. J. Biochem.* **268**, 6486–6491 (2001).
45. V. B. Borisov, R. B. Gennis, J. Hemp, M. I. Verkhovsky, The cytochrome bd respiratory oxygen reductases. *Biochim. Biophys. Acta* 1807, 1398–1413 (2011).
46. H. B. Gray, J. R. Winkler, Hole hopping through tyrosine/tryptophan chains protects proteins from oxidative damage. *Proc. Natl. Acad. Sci. U.S.A.* **112**, 10920–10925 (2015).
47. J. Chen, M. Strous, Denitrification and aerobic respiration, hybrid electron transport chains and co-evolution. *Biochim. Biophys. Acta* 1827, 136–144 (2013).
48. H.-Y. Chang, J. Hemp, Y. Chen, J. A. Fee, R. B. Gennis, The cytochrome ba3 oxygen reductase from Thermus thermophilus uses a single input channel for proton delivery to the active site and for proton pumping. *Proc. Natl. Acad. Sci. U.S.A.* **106**, 16169–16173 (2009).
49. M. R. A. Blomberg, P. E. M. Siegbahn, Why is the reduction of NO in cytochrome c dependent nitric oxide reductase (cNOR) not electrogenic? *Biochim. Biophys. Acta* 1827, 826–833 (2013).
50. M. Wikström, V. Sharma, Proton pumping by cytochrome c oxidase–A 40 year anniversary. *Biochim. Biophys. Acta* 1859, 692–698 (2018).
51. P. Y. Camejo, B. O. Oyserman, K. D. McMahon, D. R. Noguera, Integrated omic analyses provide evidence that a "Candidatus Accumulibacter phosphatis" strain performs denitrification under microaerobic conditions. *mSystems* **4**, e00193-18 (2019).
52. Y.-M. Huang, D. Straub, N. Blackwell, A. Kappler, S. Kleindienst, Meta-omics reveal Gallionellaceae and Rhodanobacter species as interdependent key players for Fe(II) oxidation and nitrate reduction in the autotrophic enrichment culture KS. *Appl. Environ. Microbiol.* **87**, e00496-21 (2021).
53. C. Brochier-Armanet, E. Talla, S. Gribaldo, The multiple evolutionary histories of dioxygen reductases: Implications for the origin and evolution of aerobic respiration. *Mol. Biol. Evol.* **26**, 285–297 (2009).
54. C. Castelle *et al.*, A new iron-oxidizing/O2-reducing supercomplex spanning both inner and outer membranes, isolated from the extreme acidophile acidithiobacillus ferrooxidans. *J. Biol. Chem.* **283**, 25803–25811 (2008).
55. J. Castresana, M. Saraste, Evolution of energetic metabolism: The respiration-early hypothesis. *Trends Biochem. Sci.* **20**, 443–448 (1995).
56. A. Loullis, E. Pinakoulaki, Probing the nitrite and nitric oxide reductase activity of cbb3 oxidase: Resonance Raman detection of a six-coordinate ferrous heme–nitrosyl species in the binuclear b3/CuB center. *Chem. Commun.* **51**, 17398–17401 (2015).
57. F. J. Stewart, O. Ulloa, E. F. DeLong, Microbial metatranscriptomics in a permanent marine oxygen minimum zone. *Environ. Microbiol.* **14**, 23–40 (2012).
58. T. Kalvelage *et al.*, Aerobic microbial respiration in oceanic oxygen minimum zones. *PLoS One* **10**, e0133526 (2015).
59. E. J. Zakem, A. Mahadevan, J. M. Lauderdale, M. J. Follows, Stable aerobic and anaerobic coexistence in anoxic marine zones. *ISME J.* **14**, 288–301 (2020).
60. V. R. I. Kaila, M. Wikström, Architecture of bacterial respiratory chains. *Nat. Rev. Microbiol.* **19**, 319–330 (2021).
61. P. G. Falkowski, T. Fenchel, E. F. Delong, The microbial engines that drive earth's biogeochemical cycles. *Science* **320**, 1034–1039 (2008).
62. J. J. R. Fraústo da Silva, R. J. P. Williams, *The Biological Chemistry of the Elements* (Clarendon–Press, 1991).
63. R. J. P. Williams, J. J. R. F. da Silva, *The Natural Selection of the Chemical Elements* (Clarendon-Press, 1996).
64. R. J. P. Williams, J. J. R. Fraústo da silva, Evolution was chemically constrained. *J. Theor. Biol.* **220**, 323–343 (2003).
65. M. M. Pereira *et al.*, The caa3 terminal oxidase of the thermohalophilic bacterium Rhodothermus marinus: A HiPIP:oxygen oxidoreductase lacking the key glutamate of the D-channel. *Biochim. Biophys. Acta* **1413**, 1–13 (1999, 1413,).
66. E. A. Berry, B. L. Trumpower, Simultaneous determination of hemes a, b, and c from pyridine hemochrome spectra. *Anal. Biochem.* **161**, 1–15 (1987).
67. R. Murali, Curated Hidden Markov Models for the heme-copper oxidoreductase superfamily. HCO HMMs. https://github.com/ranjani-m/HCO. Deposited 7 June 2022.

Materials and Methods

Growth and Expression Conditions

Rhodothermus marinus DSM 4252 was inoculated from frozen stock and grown in 5 ml of DSM Medium 630 with 10 g/L NaCl at 60 °C for 36 hrs. It was then inoculated into a larger secondary culture and grown overnight. 25 ml of the culture was inoculated into 1 L of medium with 30 mM nitrate added. The cells were shaken at 75 rpm and grown at 60 °C. The cells were pelleted by centrifugation at 8000 rpm. The cell pellet was either directly used for protein purification or frozen at -80 °C until the time of use.

Labeled ^{15}NO experiments

We used labeled nitrate ($^{15}NO_3^{2-}$) to verify that *Rhodothermus marinus* DSM 4252 was capable of complete denitrification (NO_3^- to N_2) using eNOR as the sole nitric oxide reductase. Cultures were inoculated into flasks containing media with either $^{14}NO_3^{2-}$, $^{15}NO_3^{2-}$, or no nitrate. The cultures were then allowed to grow microaerobically for a period of time before being subsampled for transfer to sealed vials in order to allow accumulation of gaseous end products. Samples were taken from each media composition after 0, 3, 6, 10, and 17 hours. The headspace was sampled after 20 hours of growth in sealed vials via gastight GC syringe and immediately injected into a Hewlett Packard 5972 gas chromatograph/mass spectrometer. Chromatogram peaks corresponding to isotopologues of NO, N_2O, and N_2 were identified by their mass spectra and peak areas were quantified relative to ambient air. As ^{15}N cultures were grown in isotopically pure $^{15}NO_3^{2-}$, complete denitrification should result in accumulation of $^{30}N_2$ at a 1:2 ratio relative to nitrate consumption. $^{30}N_2$ should only accumulate if eNOR is functioning as part of a complete denitrification pathway. If eNOR does not function effectively as a nitric oxide reductase, then ^{15}NO should be seen to accumulate. Instead, only the $^{30}N_2$ peak was observed, indicating the eNOR functioned effectively as a nitric oxide reductase for denitrification. Over the course of incubations, $^{30}N_2$ was seen to accumulate to more than 50x background. ^{14}N samples showed no significant accumulation of $^{30}N_2$ above background, confirming that the $^{30}N_2$ in ^{15}N samples was due to denitrification of labeled nitrate. NO was not seen to accumulate in any of the cultures. These results demonstrate that eNOR is a functional nitric oxide reductase and can be used as part of a complete denitrification pathway.

Purification of eNOR

The culture of *Rhodothermus marinus*, once harvested, was re-suspended in 100 mM Tris-HCl, pH 8 with 10 mM $MgCl_2$ and 50 µg/ml DNase, using a Bamix homogenizer. The homogenized cell lysate was passed through a Microfluidizer (from Microfluidics) cell at 100 psi, three times, to lyse the cells. The soluble fraction of the lysate was then separated from the insoluble by spinning down the lysate at 8000 rpm. The resulting supernatant was spun down at 42000 rpm in a Beckman Ultracentrifuge. The membrane pellet was collected and re-suspended in 20 mM Tris-HCl, pH 7.5, 1 % CHAPS (Affymetrix) to a final concentration of 40-50 mg/ml. The solution was stirred at 4 °C for 1 hr. In this step a lot of peripheral membrane proteins appear to be solubilized and the remaining protein is pelleted by spinning down at 42000 rpm for 1 hr. The remaining pellet is then solubilized in 20 mM Tris-HCl, pH 7.5, 1 % DDM (Affymetrix) at a final protein concentration of around 5-10 mg/ml. The DDM solubilized fraction was once again centrifuged at 42000 rpm to pellet down protein that was not solubilized.

The solubilized protein was then loaded on a DEAE CL-6B (Sigma) column, pre-equilibrated in 20 mM Tris-HCl, pH 7.5, 0.05 % DDM, and subjected to a linear gradient spanning from 0 to 500 mM NaCl. The fraction containing the eNOR, identified using a peak at 591nm, corresponding to the peak of cytochrome 'a1' in *Magnetospirillum magnetotacticum*(*1*), eluted at around 200 mM salt. This fraction was then loaded on a Q Sepharose High Performance (GE Healthcare) column, pre-equilibrated with 20 mM Tris-HCl, pH 7,5, 0.05 % DDM and then eluted in a gradient from 0 to 1 M NaCl. The eNOR containing fraction was eluted at around 250 mM salt and the eluted fraction was then loaded on a Chelating Sepharose (GE Healthcare) column, loaded with Cu^{2+} and equilibriated with 20 mM Tris-HCl, 500 mM NaCl, as previously described for cytochrome caa_3 from *Rhodothermus marinus*(*2*). The eNOR fraction was once again loaded on a Q

Sepharose High performance column, and a gradient was run between 0 and 300 mM NaCl at low flow rates (0.5 ml/min) and the first peak was found to be the eNOR.

Gel Electrophoresis

The purified eNOR was run on a Tris-Hepes 4-20 % acrylamide gel (NuSep) in the recommended Tris-Hepes-SDS running buffer at 120 V for ~1 hr. The protein was visualized and compared to the Precision Plus Protein™ Dual Color Standards (BIO-RAD).

UV-Visible Spectroscopy

All spectra were recorded on a HP Agilent 8453 UV-Vis spectrophotometer using a quartz cuvette from Starna Cells (No. 16.4-Q-10/Z15). Potassium Ferricyanide was used to obtain the oxidized spectrum, and dithionite was used to obtain the reduced spectrum.

Pyridine Hemochrome Assay

The hemes in eNOR were analyzed using a pyridine hemochrome assay(*3*). A stock solution of 200 mM NaOH with 40 % pyridine was prepared. The stock solution was mixed 1:1 with the protein and an oxidized spectrum was obtained by adding 3 µl of 100 mM $K_3Fe(CN)_6$. A reduced spectrum was similarly prepared by adding a few crystals of sodium dithionite. The reduced minus oxidized spectrum was used to identify the heme co-factors

Heme extraction and HPLC Analysis

The hemes from eNOR were extracted and analyzed using an HPLC elution profile according to established protocols(*4*, *5*). 50 µl of eNOR was mixed with 0.45 ml of acetone / HCl (19:1) and incubated for 20 minutes at room temperature after shaking. The mixture was centrifuged at 14,000 rpm for 2 minutes, followed by addition of 1 ml of ice cold water, and 0.3 ml of 100% ethyl acetate to the supernatant. The water/ethyl acetate mixture was vortexed and centrifuged again for 2 minutes. The ethyl acetate phase was recovered and concentrated using a speed vac.

The extracted hemes were analyzed using an Agilent 1290 Infinity LC attached to an Agilent 6230 TOF LC/MS equipment by separation using an Agilent Eclipse Plus C18 column (2.1x300 mm, 1.8 µm, 600 bar) and an acetonitrile (0.05 %TFA) / water (0.05 % TFA) gradient from 20 to 95 %.

NO reductase activity verification using GC

Anaerobic reaction conditions were set up in a 5 mL clear serum vial (Voigt Global Distribution, Inc) sealed with a 20 mm rubber stopper, by passing N_2 through 2 ml of 20 mM KPi, 0.05 % DDM, pH 7.5 with 1 mM TMPD, 5 mM Ascorbate. A control was performed by adding only 50 µM NO. Sample reactions were begun by adding eNOR to a final concentration of 100 nM. The reaction was incubated at 42 °C for half an hour before the headspace was injected into an HP Agilent 5890 Series GC, fitted with a TCD and ECD (SRI Instruments) for verification of N_2O production.

For assessment of in-vivo NO reduction activity, 5 mL of culture from actively growing *Rhodothermus marinus* in 1L of medium was incubated at 42 °C for 30 minutes in a stoppered serum vial with N_2 headspace. For each time point (at 18, 21.5 and 28 hours) 5 mL incubations of *R. marinus* culture was incubated with or without acetylene, a known inhibitor of nitrous oxide reductase. At the end of the 30 minute incubation, between 0.1 and 1 mL of headspace was injected into the HP Agilent 5890 Series GC, fitted with a TCD and ECD (SRI Instruments) for verification of N_2O production.

Turnover measurement using a Clark electrode

A sealed chamber fitted with an ISO-NO (World Precision Instruments) electrode was used for NO reductase activity measurements. 1 mM TMPD or 100 µM PMS and 4 mM Ascorbate were was added to 2 ml 50 mM Citrate, pH 6, 0.05 % DDM in the reaction chamber and all traces of oxygen were removed by

passing water-saturated Argon for 20 minutes through the solution. This is similar to the protocol described for cNOR from *Thermus thermophilus*(*6*). The buffer system also contained an oxygen scavenging system constituting 100 nM catalase, 35 nM Glucose oxidase and 90 mM Glucose. The NO reduction traces were recorded using a Duo-18 (World Precision Instruments), and activities calculated from the slope of the traces.

LC/MS/MS analysis

Mass spectrometric analysis was conducted at the Protein Sciences Facility, Roy J Carver Biotechnology Center, University of Illinois, Urbana, IL 61801 using a Thermo LTQ Velos ETD pro mass spectrometer**.** For liquid samples, the samples were cleaned up using G-Biosciences Perfect Focus (St. Louis MO) prior to digestion with trypsin. Digestion was done using proteomics grade trypsin 1:20 (G-Biosciences, St. Louis, MO) and a CEM Discover Microwave Reactor (Mathews, NC) for 15 minutes at 55° C at 50 Watts. Digested peptides were extracted 3X using 50% acetonitrile containing 5% formic acid, pooled and dried using a Speedvac (Thermo Scientific). The dried peptides were suspended in 5% acetonitrile containing 0.1% formic acid and applied to LC/MS.

HPLC for the trypsin digested peptides was performed with a Thermo Fisher Dionex 3000 RSLCnano using Thermo Acclaim PepMap RSLC column (75 µm x 15 cm C-18, 2 µm, 100Å) and a Thermo Acclaim PepMap 100 Guard column (100 µm x 2 cm, C-18, 5 µm, 100Å), solvents were water containing 0.1% formic acid (A) and acetonitrile containing 0.1% formic acid (B) at a flow rate of 300 nanoliters per minute at 40° C. Gradient was from 100% A to 60% B in 60 minutes. The effluent from the UHPLC was infused directly into a Thermo LTQ Velos ETD Pro mass spectrometer.

Control and data acquisition of the mass spectrometer was done using Xcalibur 2.2 under data dependent acquisition mode, after an initial full scan, the top five most intense ions were subjected to MS/MS fragmentation by collision induced dissociation. The raw data were processed by Mascot Distiller (Matrix Sciences, London, UK) and then by Mascot version 2.4. The result was searched against NCBI NR Protein database.

Analysis of heme-copper oxygen reductase phylogeny and distribution in environmental datasets

We performed a large-scale analysis of heme-copper oxygen reductase (HCO) protein sequences in the NCBI and IMG databases with BLASTP using an e-value of $1e^{-3}$ to generate a database of HCO sequences that had at least some of the conserved amino acids previously identified in subunit I(*7*, *8*). We then used the database of HCOs, filtered it with a sequence cut-off of 50% to generate the multiple sequence alignment, **MSA1**. A phylogenetic tree (**Fig. 2**) was inferred using IQ-TREE 2(*59*) with the substitution model VT+F+R8 and 1000 ultrafast bootstraps. Using the curated HMMs for each of the HCO family oxygen reductases (*8*, *9*), we probed release 202 of the Genome Taxonomy Database(*10*) for distribution of the NOR families – eNOR, bNOR, sNOR, nNOR, gNOR, cNOR and qNOR – in bacteria and archaea. Curated HMMs for the nitrate reductases (NapAB, NarGH), nitrite reductases (NirK, NirS) and nitrous oxide reductases (NosD and NosZ) were sourced from the HMMs database of MagicLamp(*11*).

Analysis of HCO distribution in various ecosystems were performed using the metagenomes in the IMG database. Approximately 2300 metagenomes were identified which were sourced from 44 environments identified by IMG. The number of different HCOs in each of these environments were extracted using BLASTP and query sequences that belong to each of the different HCO families.

Fig S1. Genome of *R. marinus* encodes for the complete denitrification pathway. a. The genes for NapAB, the periplasmic nitrate reductase (Rmar_0413), nitrite reductases nirK (Rmar_1208) and nirS (Rmar_0652), nitric oxide reductase eNOR(Rmar_0161) and nitrous oxide reductase, nosZ (Rmar_2012) are encoded in the *R. marinus* genome. b. The gene neighborhood of eNOR in *R. marinus*. c. The gene neighborhood of eNOR in *Magnetospirillum magneticum AMB-1* includes ctaA and ctaB, enzymes involved in the biosynthesis of heme *a*(*12*).

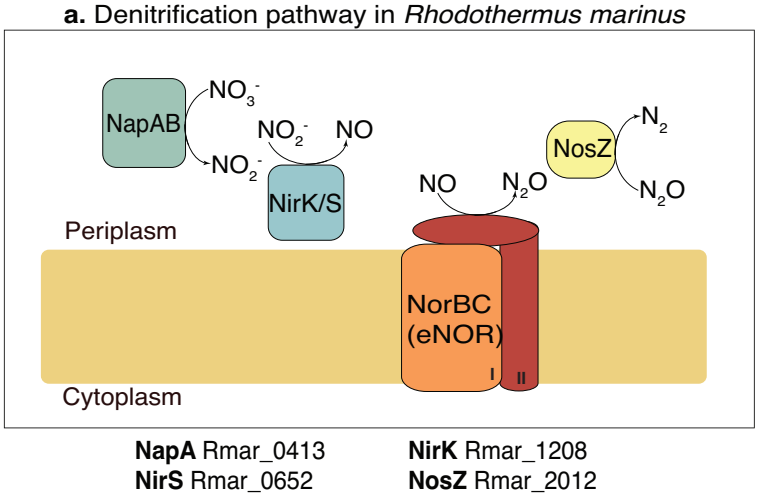

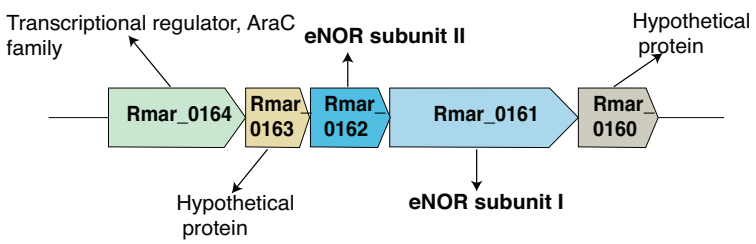

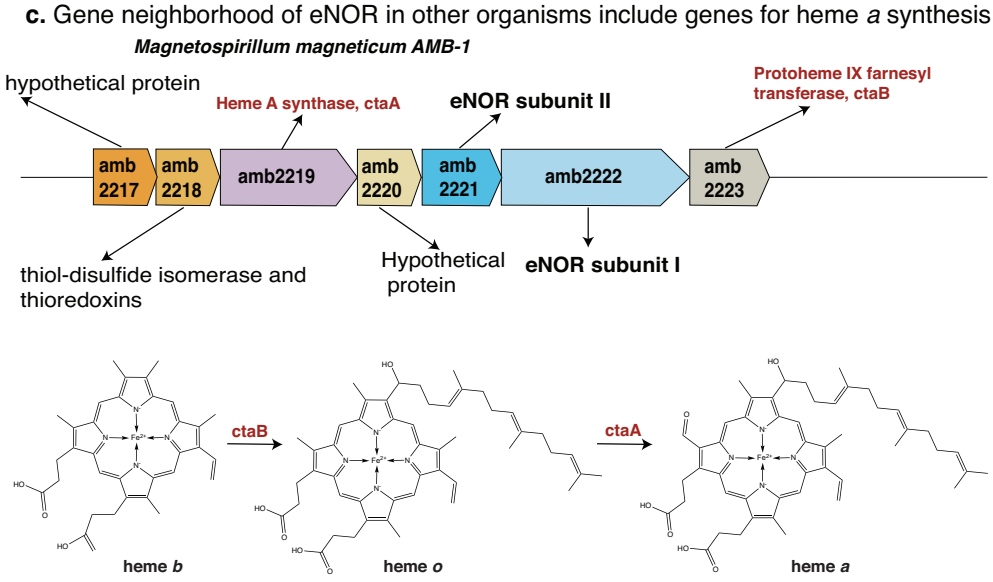

159

Fig S2: *Rhodothermus marinus* does perform complete denitrification. a. *R. marinus* converts $^{15}NO_3^-$ to $^{30}N_2$. Ratio of $^{30}N_2$ to $^{28}N_2$ for each sample. Air is ambient atmosphere as a standard. C0 is a nitrate-free control. 14 0-17 are cultures grown with unlabeled nitrate, transferred to sealed vials after 0-17 hours, respectively. 15 0-17 are the equivalent samples grown with ^{15}N-labeled nitrate. Error bars represent two standard deviations from three replicate GC/MS measurements. $^{30}N_2$ enrichments from the ^{15}N-labeled samples are over 30-60x higher than background atmospheric ratios, while unlabeled samples have no significant enrichment over background. b. Growth of *R. marinus*, measured using OD_{600nm} over 39 hours. NO_3^- utilization was established by measuring the concentrations of nitrate in the media using a calorimetric assay. c. *R. marinus* growth in rich media was compared under denitrifying and non-denitrifying conditions using OD_{600nm}. d. Phenotypic differences of *R. marinus* cultures, under denitrifying and non-denitrifying conditions.

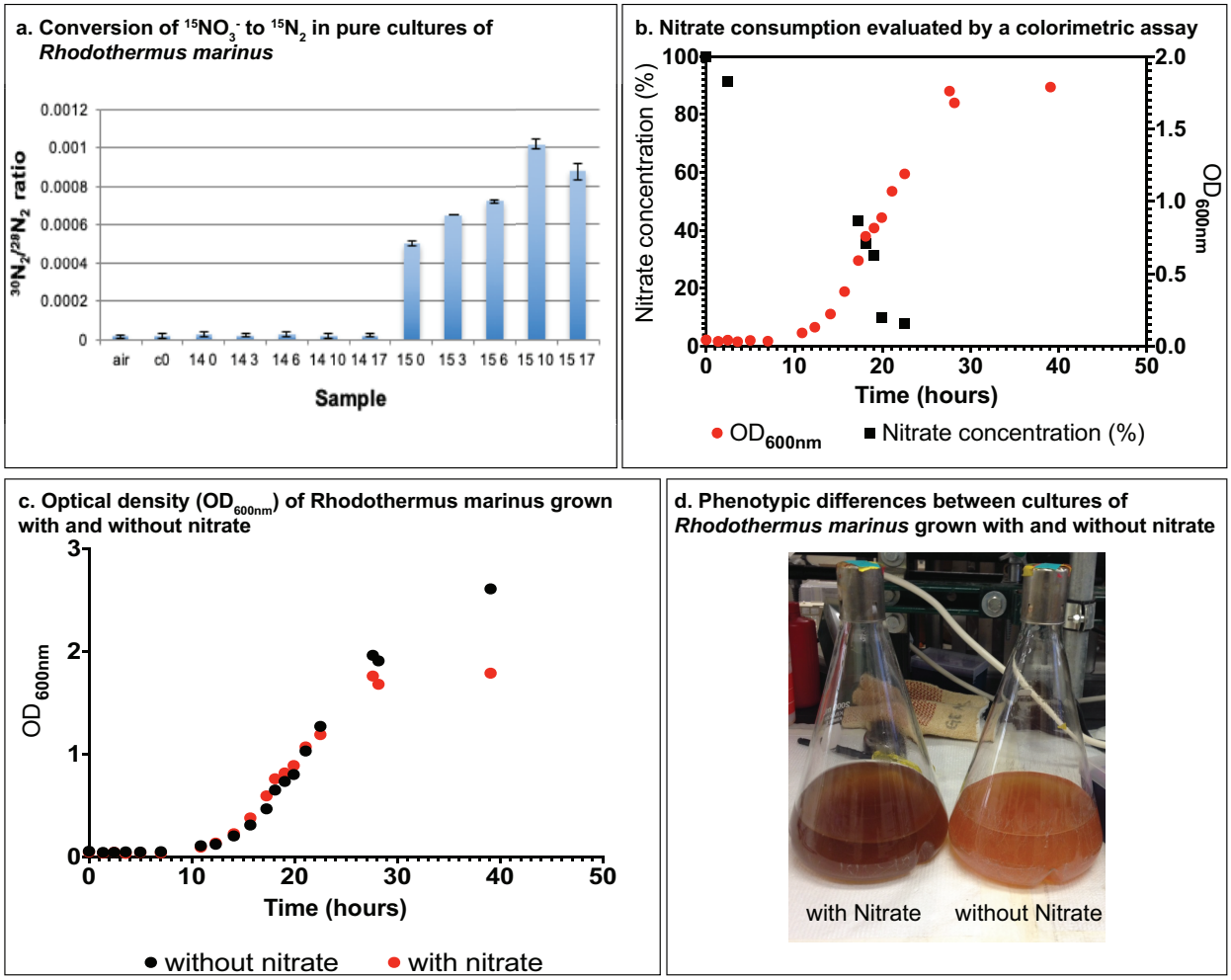

Fig S3: Characteristics of eNOR from *Rhodothermus marinus* a. SDS-PAGE gel electrophoresis of eNOR shows two bright bands which are estimated to be subunits of I and II of the complex. Both subunits appear to run faster than their estimated molecular weight. This is typical for membrane proteins. For comparison, an SDS-PAGE gel of cytochrome bo_3 oxidase from *E. coli* is included. b. Mass spectrometric identification of eNOR is confirmed by LC/MS/MS analysis. c,d. Absence of O_2 reduction by *R. marinus* eNOR, in comparison to robust O_2 reduction by *T. thermophilus* ba_3-type oxygen reductase. e. UV-visible spectrum of a membrane fraction containing eNOR f. Pyridine hemochrome-spectra of extracted hemes from eNOR showing a peak which is atypical of hemes *a, b* or *c*.

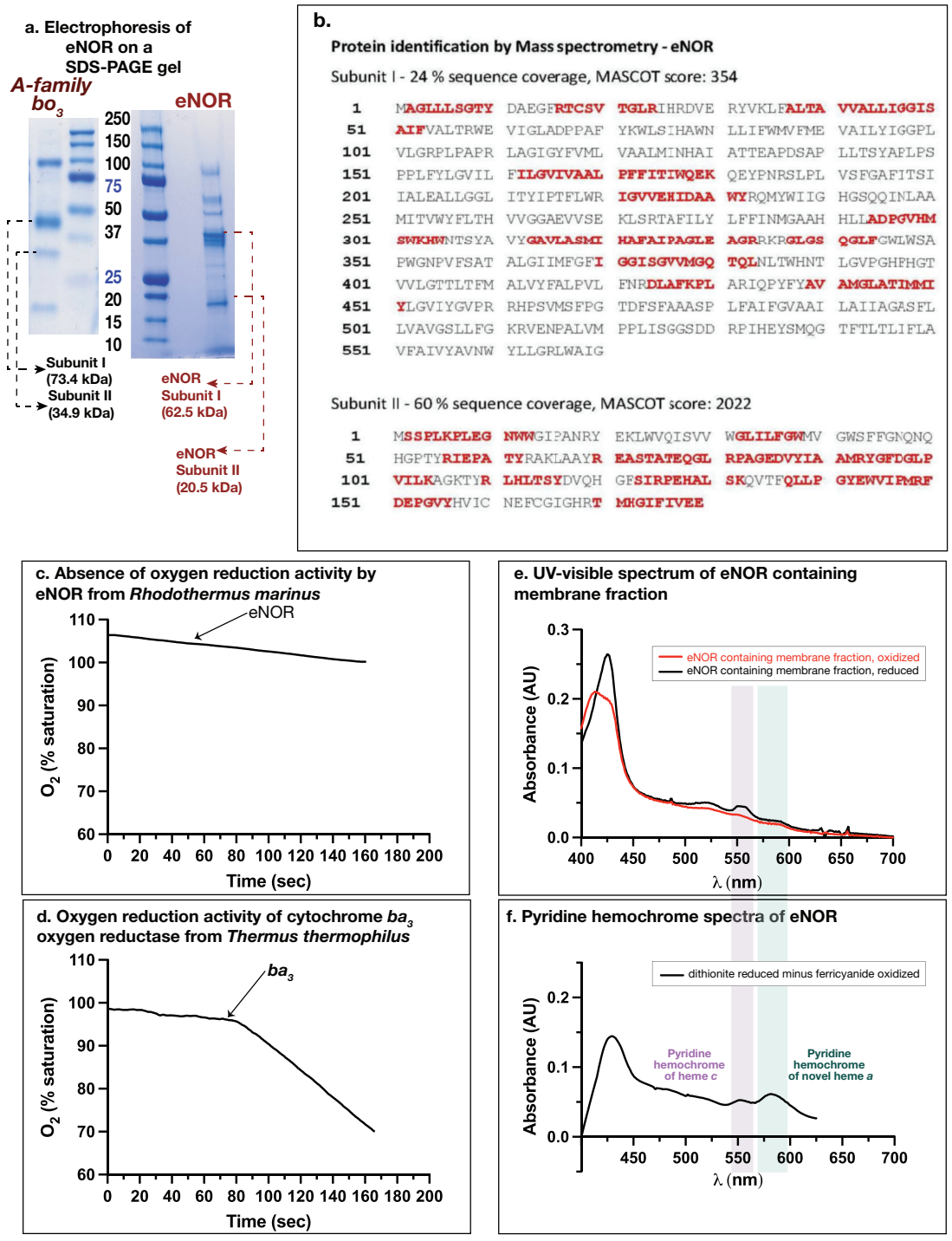

Fig S4: Identification of hemes extracted from eNOR. Comparing the elution profile of extracted hemes from partially purified *R. marinus* eNOR to bovine cytochrome *c* oxidase (A-type, t=16 min) , *T. thermophilus* ba_3-type oxygen reductase (*b*- and A_s-type hemes, t=12 min and t=19 min) reveals that the heme is most likely an A_s-type heme. Mass spectra of the peak at ~19 min from the eNOR hemes elution profile confirms that the heme is an A_s-type heme with a molecular weight of 920 Da(*13*).

a. Chemical structures of hemes A and heme As.

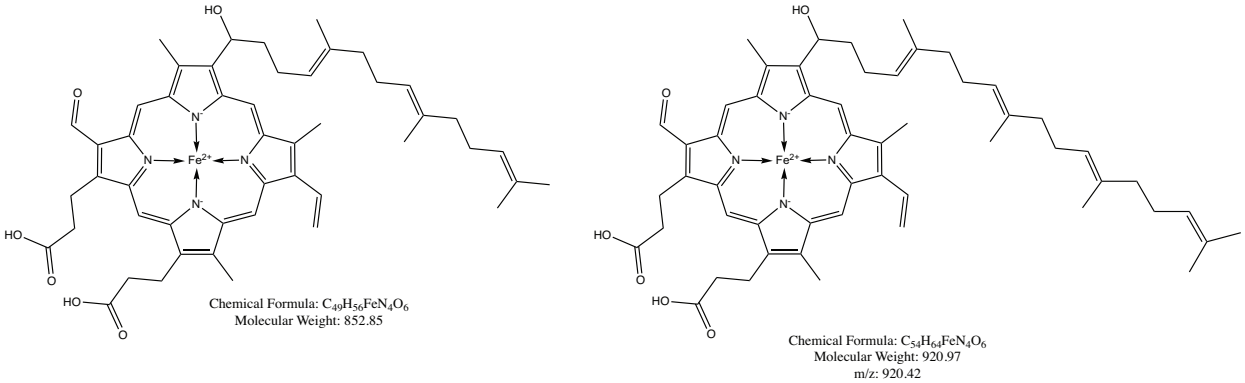

b. Elution profile of hemes extracted from eNOR (LC/MS)

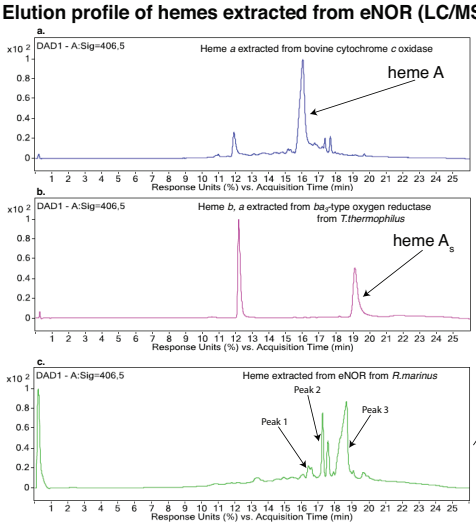

c. Mass spectra corresponding to prominent peaks in the eNOR elution profile

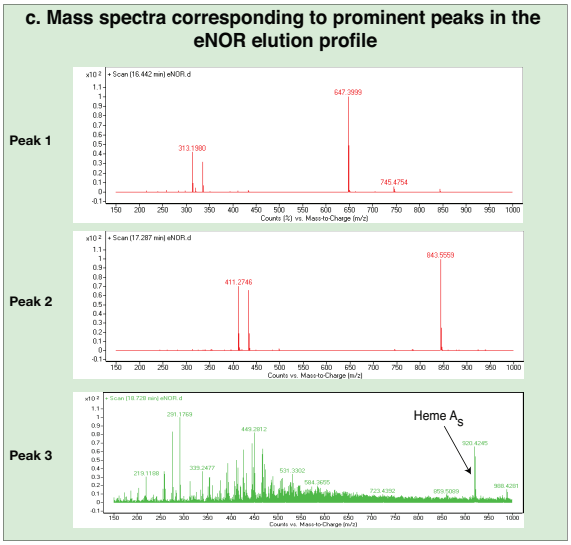

Fig S5: Proton channel in eNOR of *Rhodothermus marinus* and in the NOR families bNOR, sNOR and nNOR. a. eNOR contains conserved residues in Helix VII, similar to the location of K-proton channel residues in *T. thermophilus* ba_3-type oxygen reductase (*14*, *15*). b. A multiple sequence alignment of the NOR families eNOR, bNOR, sNOR and nNOR show conserved amino acids in an analogous location to the K-channel in the B-type oxygen reductase. Some conserved residues are also identified in gNOR and may indicate the presence of a conserved proton channel but they do not map to corresponding residues in the B-type oxygen reductase.

a. Comparison of known proton channel from ***ba*$_3$** oxygen reductase and putative proton channel in eNOR

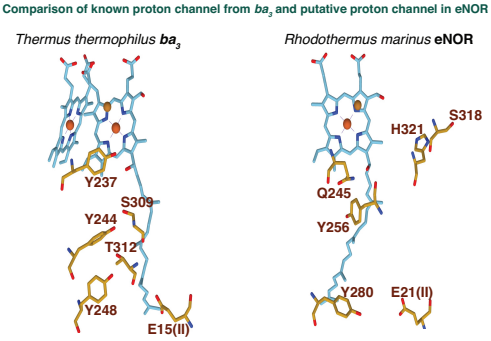

b. Conserved residues forming putative proton channels in eNOR, sNOR, bNOR and nNOR. Conserved proton channel residues are marked in black, while the active site residues are marked in **red**. Each group is numbered according to the protein whose accession number is in **blue**.

```
                                  H255 E259       Y270  Y276      Y284                H307                                T338 T341 T345
nNOR
Thermomicrobium sp002898255 GBD20489.1      FWLFAHNLMPAMGIMTLGAIYAIVPRYTR-SGQLY-SPRAAVVAMILYTMAAIPAFGHHLYTWVTGNPEVLQNVSR-STSWATGFIAATLTAFNVGLLV----------------WRNGL
Sedimenticola selenatireducens WP_084609916.1 FYIFAHNLMPAMAIMVISAVYATLPLYLADGTRKLYSDKLANLALWILLVTSVTSFFHHFYTTNPGLPSALAY-HGNFMSWATGVGAAL-STFTILATI----------------WKHGI
Sedimenticola selenatireducens PLX61751.1     FYIFAHNLMPAMAIMVISAVYATLPLYLADGTRKLYSDKLANLALWILLVTSVTSFFHHFYTTNPGLPSALAY-HGNFMSWATGVGAAL-STFTILATI----------------WKHGI
Rhodocyclaceae bacterium UTPRO2 OQY64980.1    FFFFAHNLMPAMAIMVASAIYATLPLYLADGSRKLFSDKMANLALWILLVTSITSGLHHFITFYPNQPAALSYWGS-IMSWGTGIGAAL-SIFTVFATI----------------WQHGL

                                  D285 D289       Y301                H335                                H373
gNOR
Sulfurimonas autotrophica WP_013326534.1    WWGLDLVADGLVLIYVAGSWYLLATLIT--GQKLF-MENVARAAILMLELLVSWMVWSHHLLA-DQGQPEMMKLISGEMVTAFELLTQGL-ALFITLVTL----------------WKARP
Ignavibacteria bacterium GWA2_36_19 OGU38604.1 WWGLDLIADGLVLIFVAGTWYLLATLIT--GKKLF-MENWARAALFVEMVVSWTVWSHHLMS-DQAQPGILKILSGEMVTAFELITQGL-AFFITLATL----------------WSARP
Ignavibacteria bacterium CG2_30_36_16 OIP63421.1 WWGLDLIADGLVLIFVAGTWYLLATLIT--GKKLF-MENWARAALFVEMVVSWTVWSHHLMS-DQAQPGILKILSGEMVTAFELITQGL-AFFITLATL----------------WSARP
candidate division WOR-1 bacterium OGW14262.1 WWGLDLIADGLVLIYVAGTWYLLATLIS--GKELY-MRNVARAALLVELIVSWNVWAHHLLS-DQAQPNIMKIISGEMVTAFELVTMGI-AIFITLKTL----------------WEARP
candidate division WOR-1 bacterium OGC04573.1 WWGLDLIADGLVLIYVAGTWYLLAMIIT--GRQIF-MQNFARAALFVELVVSWFVWSHHLLS-DQTQPVMMRIFSGEMITAFELVTSGI-AVFLTLATL----------------WQARP

                                  H232 N236 Y240 Y247 E248                H288                                T319
sNOR
Bacteroidetes bacterium 37-13 OJV27025.1    TFFFGHTIANEALYLGLATLYPLLPEVS--GRPKFKTTWYVALGWNCAIIFILGAFFHHLYM-DFVQPKGFQIFGQ-IASYFATIPSVVVTIISIVTLL----------------YNNKI
Geobacillus sp. WP_023634191.1              IYAFGHIFANSVIYMGVIAVYPILPKYT--NRP-WKSYKIFLIAWNMSTLFTIIIYPHHLLM-DFVMPK-WMLIIGQVFSYLNGLPVLVVTAFGALMIV----------------YRSGI
Rhodanobacter denitrificans WP_015448124.1    IYWFGHMVINATIYMGVIAVYPLLPRYT--GRP-YGISRPFLWSWAASTVFVLIVFPHHLLM-DYAEPR-WMLVMGQIISYAAGFPVFLVTAYGVLTNI----------------HRSGL
Nitrosococcus halophilus WP_013031504.1      IYFFGHVFINATIYASVTAVYPLLPRYT--GRP-WKTSKVFYAAWLAIVFMVMAVYPHHLMM-DFAMPP-WALIVGQVLSYGSGVPVMVVTGYGALMIV----------------YRSGI
Thioalkalivibrio sp. ALRh WP_019592254.1     TYFFGHVFINATIYMAVIGVYPILPRYT--GRP-WKVSRVFLAAWAASTVMVLLVYPHHLLM-DFSQPTSLHVLGQ-VISYTSGLPVLLVTAWGALTNV----------------YRSGI

                                  H233 N237 Y240      Y248                H281                                S309 T312
bNOR
Salinicoccus qingdaonensis WP_092985759.1   FWAFGHTLVNVWYLVAVSAWYLVVPKVI--GGKLF-SDSLARAVVILIVVLNVPGGFHHQIV-DPGFTEGLKFMHL-FMSLAIAVPSLL-TAFALFATLERTGRRRG-G-KGLLGWFWKL
Salinicoccus sp. YB14-2 WP_092985759.1       FWAFGHTLVNVWYLVAVSAWYLVVPKVI--GGKLF-SDSLARAVVILIVVLNVPGGFHHQIV-DPGFTEGLKFMHL-FMSLAIAVPSLL-TAFALFATLERTGRRRG-G-KGLLGWFWKL
Jeotgalicoccus psychrophilus WP_026860023.1  FWSFGHTLVNVWYLVAVSAWYIVLPKVI--GGKIF-SDSLARLVVILIVILNVPGGFHHQIV-DPGFTEGLKFMHL-FMSLAIGFPSLM-TAFALFATLERAGRNKG-G-KGLFGWFFKL
Virgibacillus dakarensis WP_088049698.1     FWSFGHTLVNIWYIVATSAWYVVVPKII--GGRVF-SDKLARLVVVLLVILNIPGGFHHQII-DPGISESVKFLHV-FMSISIAFPSLM-TAFAMFAVFERAGRKLG-G-KGLLGWFKKL
Sporosarcina sp. HYO08 KXH87068.1            FWSFGHTLVNIWYLTAVSAWYTIVPKII--GGRRF-SDTLTRVVVILLVITNIPGGFHHQIV-DPGMGEALKYMHV-FMSLAIGFPSLM-TAYAMFSVFERTGRLKG-G-KGLLGWFKKL
Sporosarcina ureilytica WP_075529285.1       FWSFGHTLVNIWYLTAVSAWYVVIPKII--GGKRF-SDTLTRVVVAMLVITNIPGGFHHQIV-DPAMGPALKYMHV-FMSLSIAFPSLM-TAFAMFYVFERTGRAKG-G-KGLFGWLKKL
Bacillus sp. FJAT-27445 WP_059173536.1       FWAFGHTLVNIWYLTAVSAWYVIIPKLM--GGRRW-SDTLTRVVVIIALVVMNITGGFHHQIV-DPGITESVKFMHV-FMSLAIGFPSLM-TAYALFAVFEKTARRNG-G-KGILGWYKKM
Bacillus sp. EB01 WP_043932172.1            FWAFGHTLVNIWYLTATSAWYVVIPKLM--GGKRW-SDTLTRVVIISLVVMNITGGFHHQIV-DPGISEAVKYMHV-FMSLAIGFPSLM-TAYALFATFEKTARRNG-G-KGLVGWYKKM
Thalassobacillus cyri WP_093046123.1         FWAFGHTLVNIWYMTAISAWYVFVPKII--DGRRW-SDMLTRIVVIALVIMNITGGFHHQII-DPGISESVKYMHV-FMSLAIGFPSLM-TAYAMFAVFEKTARKKG-G-RGLVGWYKKM
Neobacillus bataviensis WP_007083088.1       FWAFGHTLVNIWYLTAVSAWYVIVPKII--SGKRW-SDTLTRVVIIALVVMNITGGFHHQIV-DPGISPSVKFMHV-FMSLAIGFPSLM-TAWAMFAVFERTARKQG-G-KGLIGWYKKM

                                  H241 Q245 N247      Y256                Y280      H290                S318 H321
eNOR
Rhodothermus marinus WP_012842681.1          YWIIGHGSQQINLAAMITVWYFLTHVVG--GAEVV-SEKLSRTAFILYLFFINMGAAHHLLA-DPGVHMSWKHWNTSYAVYGAVLASMI-HAFAIPAGLEAGRRKRGLGSQGLFGWLWSA
Alicycliphilus denitrificans WP_013520406.1   WWAFGHSSQQINVAAHISIWYAVAAIAF--GAKPM-SERVSRGAFLLYILFLQLASAHHILA-DPGVSTEWKIVNTSYFMYFAVLGSMI-HALSIPGAMEVAQRAKGYN-KGLFEWLRKA
Candidatus Kryptonium thompsoni WP_075426648.1 FWGFGHPAQQINLAAMVSVWYLLSYFTV--GGVTP-SEKVSRTAFLLYVLFINAGSAHHLLV-DPGFGAPWKIFNTSYVIYMAVLASLI-HCFAIPASAEIGQRKRGFN-KGLFTWLIKA
Bacteroidetes bacterium OLB11 KXK43645.1        WWGLGHSSQQINVAAMVSIWYMVSFLAV--GGTSI-NEKVSRSAFVLYILFICLASAHHLLT-DPGVSSAWKVWNTSYAMYLAVLASMI-HAFAVPSSFESAQRRWGYN-KGLFEWLSKA
Gemmatimonadetes bacterium SCN 70-22 ODT01569.1 WWGLGHSSQQINVAAMVAIWYMLAALTV--GGVVL-NEKVSRSAFVLYILFISMASAHHLLV-DPGFGPAWKIVNTSYFMYMAVLASMI-HGFTVPAGMELGMRLRGYT-DGLFGWLRRA
```

Fig S6: Conserved amino acids in the eNOR family of enzymes. Multiple sequence alignment of 23 eNOR sequences from various taxonomically divergent organisms reveals conserved residues that correspond to the active site ligands, proton channel residues and other sequence features that are unique to eNOR. The active site residues are highlighted in maroon while the proton channel residues are highlighted in blue.

a. Sequence alignment of eNOR - Subunit I showing conserved amino acid residues according to *R.marinus* eNOR numbering

References

1. H. Tamegai, T. Yamanaka, Y. Fukumori, Purification and properties of a ‘cytochrome a1’-like hemoprotein from a magnetotactic bacterium, Aquaspirillum magnetotacticum. *Biochim. Biophys. Acta BBA - Gen. Subj.* **1158**, 237–243 (1993).

2. M. M. Pereira, M. Santana, C. M. Soares, J. Mendes, J. N. Carita, A. S. Fernandes, M. Saraste, M. A. Carrondo, M. Teixeira, The caa3 terminal oxidase of the thermohalophilic bacterium Rhodothermus marinus: a HiPIP:oxygen oxidoreductase lacking the key glutamate of the D-channel. *Biochim. Biophys. Acta BBA - Bioenerg.* **1413**, 1–13 (1999).

3. E. A. Berry, B. L. Trumpower, Simultaneous determination of hemes a, b, and c from pyridine hemochrome spectra. *Anal. Biochem.* **161**, 1–15 (1987).

4. N. Sone, Y. Fujiwara, Haem O can replace haem A in the active site of cytochrome c oxidase from thermophilic bacterium PS3. *FEBS Lett.* **288**, 154–158 (1991).

5. B. Reinhold-Hurek, I. B. Zhulin, Terminal oxidases of Azoarcus sp. BH72, a strictly respiratory diazotroph. *FEBS Lett.* **404**, 143–147 (1997).

6. L. A. Schurig-Briccio, P. Venkatakrishnan, J. Hemp, C. Bricio, J. Berenguer, R. B. Gennis, Characterization of the nitric oxide reductase from Thermus thermophilus. *Proc. Natl. Acad. Sci. U. S. A.* **110**, 12613–12618 (2013).

7. J. Hemp, R. B. Gennis, "Diversity of the Heme–Copper Superfamily in Archaea: Insights from Genomicsand Structural Modeling" in *Bioenergetics: Energy Conservation and Conversion*, G. Schäfer, H. S. Penefsky, Eds. (Springer, Berlin, Heidelberg, 2008; https://doi.org/10.1007/400_2007_046), *Results and Problems in Cell Differentiation*, pp. 1–31.

8. R. Murali, J. Hemp, R. B. Gennis, Evolution of quinol oxidation within the heme-copper oxidoreductase superfamily. *Biochim. Biophys. Acta BBA - Bioenerg.* **1863**, 148907 (2022).

9. R. Murali, J. Hemp, V. Orphan, Y. Bisk, FIND: Identifying Functionally and Structurally Important Features in Protein Sequences with Deep Neural Networks. *bioRxiv*, 592808 (2019).

10. D. H. Parks, M. Chuvochina, D. W. Waite, C. Rinke, A. Skarshewski, P.-A. Chaumeil, P. Hugenholtz, A standardized bacterial taxonomy based on genome phylogeny substantially revises the tree of life. *Nat. Biotechnol.* **36**, 996–1004 (2018).

11. A. Garber, MagicLamp: toolkit for annotation of ’omics datasets using curated HMM sets. (2020), (available at https://github.com/Arkadiy-Garber/MagicLamp.).

12. K. R. Brown, B. M. Allan, P. Do, E. L. Hegg, Identification of Novel Hemes Generated by Heme A Synthase: Evidence for Two Successive Monooxygenase Reactions. *Biochemistry*. **41**, 10906–10913 (2002).

13. M. Lübben, K. Morand, Novel prenylated hemes as cofactors of cytochrome oxidases. Archaea have modified hemes A and O. *J. Biol. Chem.* **269**, 21473–21479 (1994).

14. H.-Y. Chang, J. Hemp, Y. Chen, J. A. Fee, R. B. Gennis, The cytochrome ba3 oxygen reductase from Thermus thermophilus uses a single input channel for proton delivery to the active site and for proton pumping. *Proc. Natl. Acad. Sci.* **106**, 16169–16173 (2009).

15. H.-Y. Chang, S. K. Choi, A. S. Vakkasoglu, Y. Chen, J. Hemp, J. A. Fee, R. B. Gennis, Exploring the proton pump and exit pathway for pumped protons in cytochrome ba3 from Thermus thermophilus. *Proc. Natl. Acad. Sci.* **109**, 5259–5264 (2012).

Supplementary Tables

Dataset S1. Putative proton channels in the new NOR families – eNOR, bNOR, sNOR, nNOR. A list of conserved residues is noted in the table for each family with a reference sequence according to which the residues are numbered. These conserved residues are compared with amino acids found in analogous positions in the B-type oxygen reductase. (available as an .xlsx file in online supplementary material). (.xlsx)

Dataset S2. Multiple sequence alignment of HCO superfamily. Multiple sequence alignment of sequences from families of the heme-copper oxidoreductase superfamily were aligned using MUSCLE. Various families are grouped when visualized in Jalview and amino acids are colored using a ClustalX algorithim with a greater than 90 % identity. This alignment was manually curated to improve the alignment and reduce the number of gaps. (.pdf)

Dataset S3. Newick treefile for the phylogenetic tree of the HCO superfamily depicted in Figure 2 made available as a pdf. (.pdf)

Dataset S4. Leaf labels from the phylogenetic tree of the HCO superfamily depicted in Figure 2. (.xlsx)

Dataset S5. Conserved tryptophan/tyrosine residues in NOR families from the HCO superfamily. Conserved tryptophan/tyrosine residues identified in NOR families that may form a tryptophan/tyrosine chain that allows for the movement of free-radicals to the surface of proteins to allow for their quenching by redox-active molecules in the cell, without damaging the protein. (.xlsx)

Dataset S6. Distribution of HCO sequences in GTDB. A distribution of all the NOR families within various bacterial and archaeal species within the genomes in release 202 of GTDB was analyzed using HMMs that are specific to each NOR family. (available as an .xlsx file in online supplementary material). (.xlsx)

Dataset S7. Distribution of NOR families in various ecosystems as per the IMG database. A distribution of various NOR families in over 2000 metagenomes on the IMG database was evaluated, and then tabulated according to the environment from which each metagenome is sourced. (available as an .xlsx file in online supplementary material). (.xlsx)

Dataset S8. Denitrification pathways in bacteria and archaea. An analysis of denitrification pathways in bacterial genomes and archaeal genomes in release 202 of GTDB was performed by searching for the presence and absence of NarGHI, NapAB, NirK, NirS, NosZ, NosD and the NORs in each genome using curated HMMs for each of the proteins. (available as an .xlsx file in online supplementary material). (.xlsx)